land

MDPI

Article

Development of an ArcGIS-Pro Toolkit for Assessing the Effects of Bridge Construction on Overland Soil Erosion

Habib Ahmari *, Matthew Pebworth, Saman Baharvand, Subhas Kandel and Xinbao Yu

Department of Civil Engineering, The University of Texas at Arlington, Arlington, TX 76010, USA
* Correspondence: habib.ahmari@uta.edu

Abstract: Erosion is a natural process, but it can be accelerated by anthropogenic activities. Two of the predominant types of human-induced erosion are related to agricultural and construction activities. Of the two, construction-induced erosion is more severe because of the simultaneous removal of the land cover, disturbance of the soil, and eventual compaction of the soil by heavy machinery. Eroded materials released from bridge construction sites can alter the sediment regime and geomorphological conditions of receiving streams and may have short- and long-term impacts on aquatic habitats. Several models have been developed to estimate the total amount of soil erosion and sediment yield; however, no predictive model is available to quantify the potential release of sediment during the construction of bridges or to predict the quantity, size fraction, and accumulation depths for the extent of the measurable downstream effect. A GIS-based predictive sediment toolkit is developed to estimate the overland erosion and to determine the potential depositional area and suspended sediment concentration downstream of bridges. The performance of the GIS toolkit in estimating soil erosion was assessed using field data collected from the Wilson Creek bridge construction site in McKenney, Texas, U.S., and it was concluded that it predicted the overland erosion rate and sediment yield within the ranges observed in the field.

Keywords: overland erosion; bridge construction; modified universal soil loss equation; sediment yield; empirical formulas

Citation: Ahmari, H.; Pebworth, M.; Baharvand, S.; Kandel, S.; Yu, X. Development of an ArcGIS-Pro Toolkit for Assessing the Effects of Bridge Construction on Overland Soil Erosion. *Land* **2022**, *11*, 1586. https://doi.org/10.3390/land11091586

Academic Editors: Yaser Ostovari, Ali Akbar Moosavi and Deirdre Dragovich

Received: 14 August 2022
Accepted: 12 September 2022
Published: 16 September 2022

1. Introduction

Bridges are critical points of road networks, and the number of bridge construction projects is rising due to the continuous population growth that necessitates the widening of existing roads and construction of new interchanges [1]. Bridge construction activities are not limited to the actual construction of bridges but also include road widening and improvements to the associated approach lanes and sometimes reshaping of streambanks. All construction works that release sediment into streams are considered part of bridge construction activities.

The impacts of bridge construction can be classified into two categories: those that are overland and those that are on/in the water. The overland works include approach embankments, bridge abutments, retaining walls, slopes, and temporary work platforms used during the construction. The in-water works include construction of bridge elements in or above the water, such as foundations, bridge piers and decks, and cofferdams.

Construction activities disturb soil structures and vegetation covers and may accelerate the overland erosion process [2]. Activities such as the drilling of bridge foundations or in-water construction activities can result in mud being released into streams in the form of stormwater or as direct discharge. Sediment usually consists of clay, silt, and sand particles, cement wash-off, colloidal particles, and organic matter [3], and an excessive load may increase turbidity, change the stream morphology and stream bottom, and affect aquatic habitats [4,5]. The amount of sediment yield is affected by the intensity of the erosive forces and the sediment transport process. An intense storm of long duration can exacerbate soil

erosion and lead to an increase in the amount of sediment released to the receiving body of water, as can various stages of bridge construction that involve a significant amount of earthwork, including excavation, grading, and sloping. Road and bridge construction sites are the major sources of sediment in streams [6].

Several models have been developed previously to estimate overland erosion, but their use is primarily intended for agricultural purposes and their applicability to construction sites is unknown [7]. For example, the SWAT model was used to evaluate the impacts of land use changes on streamflow and sediment yield in the Atibaia River Basin, Brazil [8]. It was concluded that curve number (*CN*), maximum canopy storage, and the land cover and management factor (*C*) had the largest impacts on streamflow and sediment yield. The physics-based EROSION-3D model was applied to simulate erosion-runoff processes in the Svacenický Creek watershed, the Slovak Republic, which is composed of 66% cropland [9]. The model results were used to identify the most vulnerable erosion and depositional areas within the watershed. The ANSWERS model was used to predict runoff and soil loss from three agricultural watersheds in the arid zone of India [10]. The model inputs including landform, drainage, soil, and land use/land cover were obtained from satellite imagery and limited field data. The results showed that the model predicted runoff hydrograph and sediment load within acceptable limits. The ArcMUSLE, a GIS-based tool, was developed to assess soil erosion risk and prioritize critical areas for soil erosion control practices [11]. The model was applied to an agricultural watershed in Black Hawk County, Iowa, USA. The output of the tool includes curve number, runoff amount, peak flow, and soil loss for a rainfall event within the watershed. The widely used overland erosion models are discussed in Section 2.

A GIS-based predictive sediment toolkit (PST) was developed in this research to estimate overland erosion and to determine the potential depositional area and suspended sediment concentration downstream of bridge construction sites. The PST can also be used to assess the impact of construction activities on aquatic life. One of the biggest inconsistencies in construction-related stream assessments is the delineation of the impacted area. Environmental agencies usually define the minimum buffer length for habitat surveys. This length comprises the project footprint and buffers for areas of the potential impact that include a minimum length upstream and downstream of the project [12–15]. It is unknown whether these buffer lengths adequately protect aquatic species. Field monitoring and numerical modeling efforts have been reported in various road and bridge construction projects where attempts are made to assess construction impacts on the stream sediment regime and aquatic habitat [7]. However, no predictive model was available prior to this research to quantify the potential release of sediment during the construction of bridges.

The development of PST was based on two models: the overland erosion model (OEM) and the in-stream sediment transport model (STM). The toolkit was designed as an ArcGIS add-in with pre-populated base data for the state of Texas, U.S.; however, it can be used for any bridge construction site by importing local base data. The development of the OEM, governing equations, and application for a bridge construction site are discussed in the following.

2. Overland Erosion and Sediment Yield

Erosion is a natural process, but excessive sediment delivery due to anthropogenic activities is one of the highest threats to the health of river systems [16]. Agricultural and construction activities are two of the predominant types of human-induced erosion with construction being 100 times more severe [17] because of the simultaneous removal of the land cover, disturbance of soil, and eventual compaction of soil by heavy machinery.

Several models have been developed to estimate the total amount of watershed erosion (also known as gross erosion) and sediment yield (the portion of the eroded material that enters streams). These models can be classified as empirical, conceptual, and physics-based models [18]. In this study, the conceptual and physics-based models are grouped into

synergistic models. Some of these models and their applicability for estimating overland erosion at construction sites are discussed in the following.

2.1. Empirical Models

Universal Soil Loss Equation (USLE)

The most widely used soil erosion model, the Universal Soil Loss Equation (USLE), was originally released in 1965 and has since been used across the globe [19]. It is based on statistical analyses of data from 46 locations in more than 10 states in the central and eastern U.S. [20]. The USLE relationship has the following form:

$$A = R \times K \times LS \times C \times P \quad (1)$$

In this equation, A (tons/ha/yr.) is the soil loss, R (MJ·mm/h/ha/yr.) is the rainfall erosivity factor (which may vary seasonally and is determined via a table or R contour maps), K (tons·h/MJ/mm) represents the tendency of soil to erode, and LS (dimensionless) is obtained from established values presented in tables and represents the combined influence of slope length, or how long sediment may travel before deposition, and the slope steepness of the study area. The C factor (dimensionless) accounts for any soil coverings that impede the soil's ability to erode, especially in terms of rainfall-impacted erosivity. Organizations such as the U.S. Environmental Protection Agency (EPA) have collected ranges for C, relative to construction Best Management Practices (BMPs) [21]. The term P (dimensionless) accounts for support practices, which are activities that are designed to limit the sediment yield of an area. Further information on the USLE parameters discussed here may be viewed in their respective formats via the U.S. Bureau of Reclamation Erosion and Sedimentation Manual [22].

Since the equation is empirical, it is relatively simple to use it to estimate overland erosion. It can generate a loading prediction based on annual averaged data; however, it should not be used on a storm-by-storm basis. The model is primarily intended to calculate erosion from agricultural land and only considers sheet erosion; it neglects both rill and gully erosion. Consequently, it cannot be used for construction sites where non-agricultural areas exist, sub-yearly erosion estimates are required, and/or erosion parameters are expected to change with time.

Revised Universal Soil Loss Equation (RUSLE)

RUSLE2 is an updated form of the USLE model and the second major iteration of RUSLE itself. RUSLE2 was introduced in 1992 to address USLE's use in regions that it was not previously intended for, especially outside of the U.S. [23]. It uses the same form of relationship as the USLE but accounts for sub-yearly variations in the equation's parameters and makes use of an LS equation that replaces the tables developed previously for the USLE model. Updated maps for R values to be used in the RUSLE2 model were developed and may be found in [24] and elsewhere.

RUSLE2 uses daily values to determine the sediment annual yield and adjusts it with an equation for deposition that is presented in [20]. It considers both rill and inter-rill erosion and because it uses daily values for all components except the slope, it is more responsive to short-term changes. It also determines an annual sediment load via the summation of daily loads, meaning that it can be used to evaluate any integer daytime period. It requires both daily precipitation and temperature data to estimate the C factor, the need for which can introduce uncertainty into the calculations or require more comprehensive data to be available, both for use and to improve future temperature estimates. Daily precipitation values are derived from monthly average values, and because this model uses average rainfall values and a rainfall-erosivity factor that is directly related to intensity, such an approximation may not be ideal for short-term estimations. Since the improved accuracy of this model comes from its daily variables, if R, K, L, C, and P variables are not at the daily scale, the improvement in accuracy is reduced. The RUSLE model was not considered in this research primarily because of the need for short-term sediment load

estimates at bridge construction sites. The need for temperature data and daily values of most of the variables also contributed, to a lesser degree, to this decision. This additional information would not result in a better estimation of sediment yield, rather it adds to the list of required data that might not be available for each construction site.

Modified Universal Soil Loss Equation (MUSLE)

MUSLE is another derivation of USLE. This model, unlike both RUSLE and USLE, does not make use of the rainfall erosivity factor R; instead, it relates the sediment yield Q_s to both the storm runoff volume Q and peak q_p for a single event. This empirical relation is explicitly designed for a single storm event that has an arbitrary duration. Runoff is better linked to erosivity than rainfall [25]. It may better predict erosion in urban areas due to increased peak flows from increased imperviousness. The runoff energy factor eliminates the need for an independent deposition formula as is used in RUSLE2 [25]. This model can estimate erosion for a single storm or be used multiple times to determine daily, monthly, yearly, or total sediment loads for any construction duration. For these reasons and because of its simplicity, MUSLE was considered in developing the overland erosion model (See Section 3.1).

Younkin Model

The empirical equation proposed by Younkin [26] is the only model that has been developed to estimate the sediment supply to a stream during periods of rainfall-induced erosion of disturbed soils that are common to highway construction (Equation (2)). In this equation Q_{ss} (tons) is the suspended sediment yield at the stream station, R is the rainfall erosivity factor as defined in both USLE and RUSLE for a single storm event, A (square yards) is the area of the construction site, D (yards) is the average depth of disturbed soil, and P (dimensionless) is the ratio of the area upslope of the stream to the total area of the site.

$$Q_{ss} = 0.34\ R^{1.5}\ (\log A)^{2.45}\ (3.0)^{D}\ P^{-0.72} \quad (2)$$

In developing this equation, a total of 86 sediment data sets were collected from 5 stream locations along White Deer Creek during the construction of Interstate 80, Pennsylvania, U.S. The Younkin and USLE equations were found to perform almost identically, when compared against normal stream loading for almost 100 storm events [27]. Equation (2) is distinct from the empirical equations discussed above because it was derived using data from construction sites; however, it has not been as heavily validated as the above equations and is considered slightly inferior to more established sediment loading estimation methods [27]. The same field data set used to develop Equation (2) was utilized to validate the model performance. While it was specifically derived for construction activities, it is not well enough developed to warrant selecting it over more broadly validated equations.

2.2. Synergistic Models

Synergistic models attempt to combine various data to produce a more accurate picture of what is occurring inside a simulation domain. They are also capable of utilizing more complicated relationships. For example, they use iterative equations, such as the Green-Ampt method, to account for infiltration, sediment transport relationships, such as Shields' diagram, to calculate critical shear stress, and statistics-based methods to simulate weather. These relationships require more data, however, which adds to the computational cost and decreases the ease of using them. Some of the most widely used synergic models are ANSWERS (Areal Non-point Source Watershed Environmental Response Simulation Model) [28], EUROSEM (European Soil Erosion Model) [29], WEPP (Watershed Erosion Prediction Project) [30], and SWAT (Soil and Water Assessment Tool) [31]. These models largely focus on agricultural applications, and while some respected exceptions exist, they have a larger overall focus and are thus more complicated than necessary for estimating erosion from bridge construction sites. SWAT uses the MUSLE equation for its overland erosion calculation; however, functions such as modeling bacterial and algal growth,

nitrogen and phosphorus transport/cycles, and accounting for groundwater flows are unnecessary for estimating soil erosion from construction sites and are computationally inefficient for this application. It was designed for long-term simulations and not for single-event analysis [31].

3. Overland Erosion GIS Toolkit

A GIS-based toolkit is developed to determine the amount of overland erosion induced by runoff from bridge construction sites and to assess changes in the sediment regime of downstream waterbodies. Precipitation events are the primary cause of construction site sediment and turbidity discharges to surface waters [2]. Wind erosion is not considered in the model because bridge construction is a temporary activity with a relatively limited footprint. In addition, wind erosion mostly affects lighter soil particles and transports them as dust, whereas heavier materials settle down and result in sedimentation. Wind-blown dust from earthworks sites can be a significant form of air pollution [2].

The toolkit is designed as an ArcGIS add-in that uses a combination of base data and user-supplied information to estimate the amount of sediment released from bridge construction sites to downstream waterbodies. It is developed based on two interconnected models: the overland erosion model (OEM), and the in-stream sediment transport model (STM). The governing equations of the OEM and information that is required for estimating overland erosion in bridge construction sites are discussed in the following.

The MUSLE has been utilized extensively in many watersheds throughout the world for different purposes and has produced reasonable results when it is applied under conditions similar to those where the original formula was developed or calibrated [32]. Since it was originally developed with data from microwatersheds [25,33], it appears appropriate to use this model for bridge construction sites that usually have small contributing watersheds. It has been also argued that if the MUSEL model is used instead of USLE, the accuracy in estimating sediment yield is increased because it eliminates the need for sediment delivery ratio calculation. Moreover, all model parameters can potentially be used in the calibration and validation process, especially when the model is applied to watersheds that have different conditions than those where the model was originally developed [34]. For these reasons, the MUSLE was chosen for developing the OEM in this study.

The core of the OEM is the information it requires about hydrological conditions and soil characteristics to estimate the sediment yield from the MUSLE model. The method used by the Natural Resources Conservation Service (NRCS), formerly known as the Soil Conservation Service (SCS), relates rainfall to both peak flow rate and flow volume [35], both of which are required to utilize the MUSLE model, and uses rainfall, flow length, percent slope, storage, and the watershed area to estimate those quantities. Figure 1 displays the order in which the SCS and the MUSLE are used in the GIS toolkit. The MUSLE model and SCS method, and the input data, including supplied and user-defined data, are discussed in the following.

3.1. MUSLE Model

The MUSLE model relates soil erosivity to both stormwater runoff volume Q and peak flow q_p. It does not relate erosion to rainfall impact energy as in the original USLE because impact energy may not be useful in urban environments with increased development. The MUSLE equation is given in the following [32,34].

$$Q_s = 11.8\,(Q \times q_p)^{0.56} \times K \times LS \times C \times P \tag{3}$$

where Q_s (tonnes) represents sediment yield, Q (m^3) is the flow volume, q_p (m^3/s) refers to the peak flow rate, K (dimensionless) is soil erosivity, LS (dimensionless) is slope length factor, C (dimensionless) is the management practice factor, and P (dimensionless) is the erosion control factor. The present study used the SCS method to calculate the total flow volume and peak flow rate.

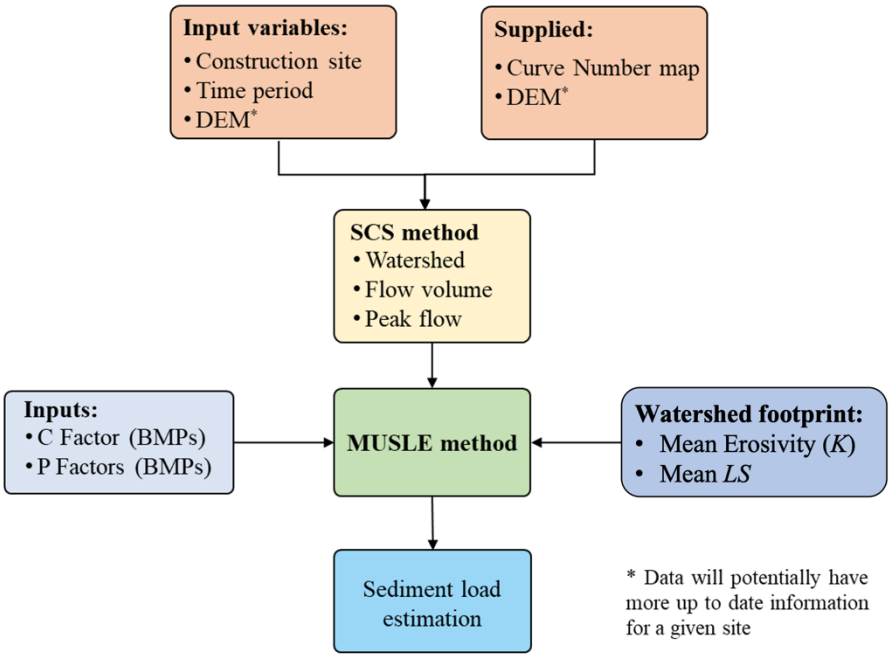

Figure 1. Overland erosion model input flowchart.

3.2. SCS Method

The SCS method was selected to estimate the runoff volume and the peak flow rate. Equations (4) and (5) are used to calculate the runoff depth P_e (mm) and the peak flow rate q_p (m^3/s) [35].

$$P_e = \frac{(P - 0.2S)^2}{P + 0.8S} \tag{4}$$

$$q_p = \frac{2.08\ A\ P_e}{0.67\ t_c} \tag{5}$$

where P (mm) is total rainfall, S (mm) is potential maximum retention, A (km^2) is the watershed area, and t_c (h) represents the time of concentration. S and t_c are calculated using Equations (6) and (7).

$$S = \frac{2540}{CN} - 25.4 \tag{6}$$

$$t_c = \frac{(3.28L)^{0.8}(Y+1)^{0.7}}{1140\ Y^{0.5}} \tag{7}$$

In these equations, CN (dimensionless) is the curve number, L (m) is the flow length, and Y (%) is the average slope along the flow path. The runoff volume is calculated as $Q = P_e\ A$.

Some of the parameters needed for the MUSLE and SCS equations cannot be populated in the GIS toolkit or manipulated prior to a simulation. For instance, the slope length factor is specific to the watershed being investigated, but it is derived from the internally supplied digital elevation model (DEM). Conversely, management and erosion control factors rely on their site-specific implementation but have a known efficiency range. Other parameters, such as existing soil erosivity (K) and both management practices (C) and erosion control (P) factors, may be pre-loaded.

3.3. Model Inputs

The OEM requires both preloaded and user-defined data to calculate the overland erosion at construction sites. The preloaded data includes the digital elevation model (DEM), curve number (CN), soil erosivity (K), soil gradation, stream segments, and road map inventory. For this research, these data were collected for the state of Texas, from

the sources that are presented in the following sections, as a base reference to be used in analyzing overland erosion, but such information for other locations can be uploaded into the model in advance. The user-defined data includes the project's footprint, start and end date of construction activities, and Best Management Practices (BMPs) that will be utilized by the contractor. Since construction activities may alter elevations, land cover, and soil type, these changes impact surface flow patterns, runoff volume and peak flow, and the overland erosion process and magnitude. Therefore, the user should introduce any changes in DEM, *CN*, and *K* due to construction activities. Rainfall is another important input to the overland erosion model, and it is synthesized by using data from the most recent 50 years obtained from the rainfall gauge closest to the bridge construction site.

3.3.1. Preloaded Data

Digital Elevation Model (DEM)

The DEM obtained from the United States Department of Agriculture NRCS gateway data [36] was assembled and then clipped with the Texas boundary; the data may be replaced by a new DEM with different resolutions, or DEM of a disturbed construction site to meet the needs of the user. The resolution of the DEM is 10 m, and finer resolutions portend higher quality analyses, but the improved hydrologic analysis comes at the cost of increased computational time. Figure 2a contains the DEM for Texas.

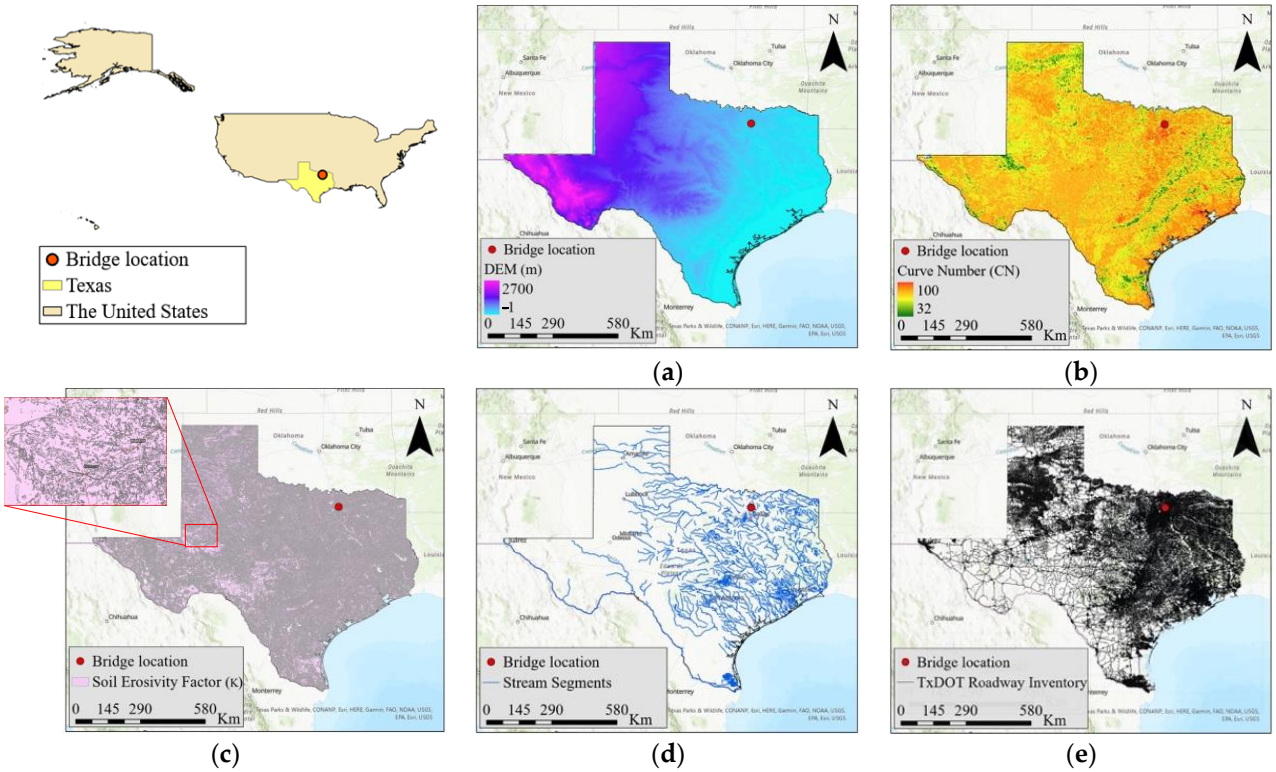

Figure 2. Pre-populated base data in the GIS toolkit for the state of Texas: (**a**) Digital elevation model (DEM), (**b**) Curve Number (*CN*), (**c**) Soil erosivity factor (*K*), (**d**) Stream segments, and (**e**) Road map inventory.

CurveNumber (CN)

The *CN* of a region is associated with its runoff potential, with higher values indicating increased potential for runoff. The curve number, as a raster, was derived from the NLCD (National Land Cover Database), hydrologic soil groups, and the DEM. The HEC-GeoHMS was used in conjunction with a table created from *CN* values retrieved from a USGS (United State Geological Survey) and Bureau of Reclamation co-authored document [37]. The *CN* map for Texas is shown in Figure 2b.

Soil Erosivity Factor (K)

The soil erosivity factor (*K*) is a shapefile that references the erosivity of the soil. *K* is intrinsic to the soil itself and is determined via properties, such as soil texture, organic material, and permeability; however, disturbance of the ground surface may warrant adjusting the values. The default values are provided in the model for undisturbed soils. The soil erosivity (*K*) was downloaded from the U.S. Department of Agriculture (USDA) web soil survey [38]. The SSURGO (Soil Survey Geographic Database) data was collected for all counties within Texas; each county file was imported and merged with the others. Using the USDA-supplied soil data viewer, the soil erosivity is exported as a GIS recognizable format. Figure 2c shows the soil erosivity shapefile, with an inset to emphasize finer details.

Stream Segments

The stream segments as line data that traces the path of waterbodies in Texas, were obtained from the TCEQ (Texas Commission on Environmental Quality) GIS data portal [39]. Stationary waterbodies, such as lakes and reservoirs, are not included in this data set, and the data was not split because of its comparatively small file size. Figure 2d shows the TCEQ stream segments.

Road Map Inventory

The GIS data for Texas roadways was downloaded from the Texas Department of Transportation (TxDOT) GIS portal [40] and contains numerous characteristics associated with the road segments they represent. For this model, the number and width of a high occupancy vehicle (HOV) and normal lanes were found and appropriately multiplied and buffered. This created a plan view of the road network footprint, neglecting internal medians, that was used to modify the *K* and *CN* values found in the data sets. Conventional paved roads are neither permeable nor readily erodible; therefore, the *K* value was set to 0.01 and the *CN* value to 99 to adjust the data sets. The TxDOT Road Map Inventory is displayed in Figure 2e.

3.3.2. User-Defined Data

The GIS toolkit interface and its data entry page are shown in Figure 3.

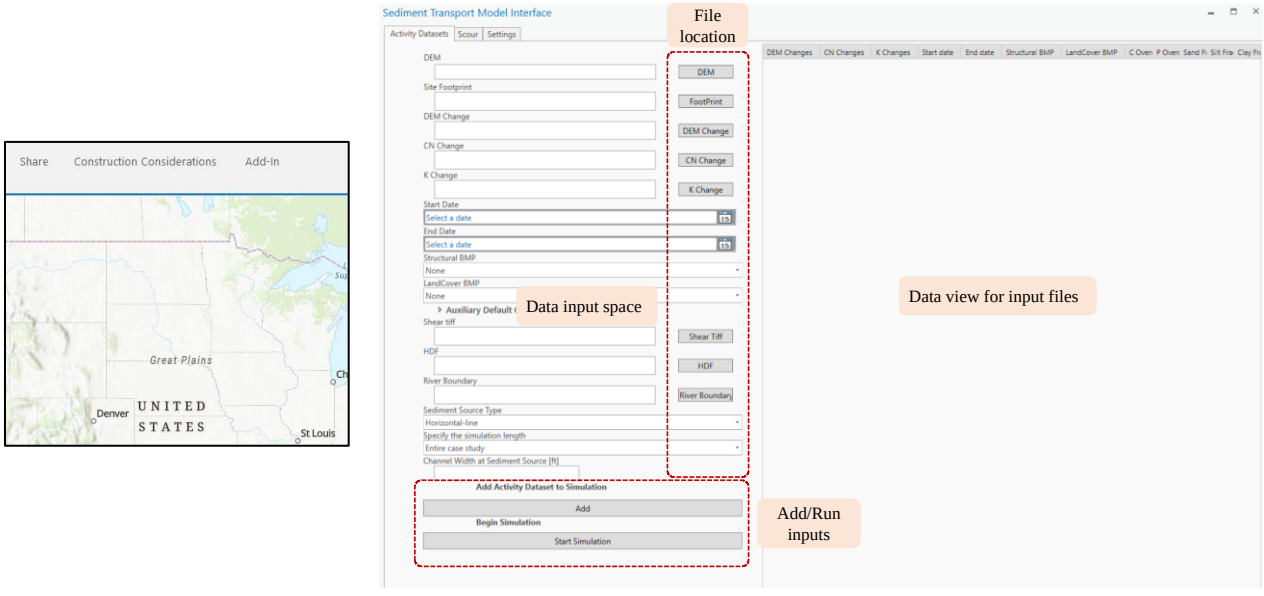

(**a**) (**b**)

Figure 3. (**a**) GIS toolkit interface, and (**b**) Data entry space.

Construction Site Footprint

This variable is a shapefile that is entirely defined by the user. While the input shapefile may be made up of multiple polygons, the model currently only looks at the point where the highest volume of runoff occurs. All hydrologic calculations and resulting sediment loads are based on the point with the greatest contributing volume and corresponding greatest contributing area.

Start and End Dates of Construction Activities

These values mark the start and end of each construction activity. The range of dates, inclusive of the ends, are included in the sediment loading point file. The date may be typed in the format mm/dd/yyyy; alternatively, the date picker may be used.

DEM Change

A DEM Change variable is provided because earthwork is a normal occurrence in construction processes, and altered elevations could change surface flow patterns. Raster resolution is required to match the resolution of input DEM. This variable is only useful when large quantities of earthwork or earthwork that exceeds a single raster cell coverage is performed. The raster input should show the expected new elevations, not the difference from the existing elevations.

Curve Number (CN) Change

Alterations in the site conditions can change how much rainfall an area may absorb and influence the runoff volume and response time. Should noteworthy changes occur, they may be input in the form of a raster that shows the expected conditions, not the difference.

Soil Erosivity Factor (K) Change

Disturbance of the ground surface due to construction activities may warrant adjusting the *K* value. Loosening or compacting soil changes the ease with which it may be carried away with runoff. The new *K* values may be in the form of polygon shapefiles. This shapefile should be prepared by the user and uploaded if the native soil in the construction area is disturbed, and foreign soil has been used in filling activities.

Best Management Practices (BMPs)

BMPs are artificial measures implemented to reduce soil erosion, sedimentation, and non-point source pollution. Different BMPs may be utilized by various sectors to achieve these goals. Examples of agricultural BMPs are conservation tillage, bench terracing, and conservation buffers. In stormwater management for urban areas, BMPs are utilized to remove pollutants from runoff. BMPs may include vegetated swales, retention/detention ponds, raingardens, and wetlands. For this research, the commonly used construction BMPs and their efficiencies were collected from documentation of completed construction projects and a literature review and were pre-assembled as two drop-down lists: structural BMPs and landscape BMPs (Figure 4). BMPs efficiency relates the performance of practice to soil loss reduction. The user may select the type and efficiency of BMPs that are to be implemented. Land management factor (*C*) and erosion control factor (*P*) in the MUSLE equation are accounted for via landscape and structural BMPs, respectively.

Structural BMPs account for discrete alterations to the construction site. Examples of structural BMPs are slope benches, silt fences, filter socks, and retention ponds. By default, this parameter is set to the *None* condition, but selecting the drop-down button allows for each construction activity. Landscape BMPs account for non-discrete alterations to the construction site. Mulching, hydroseeding, and turfing are common landscape BMPs in construction projects. By default, this parameter is set to the *None* condition, but selecting the drop-down button allows the parameter to be changed for each construction activity.

Should a BMP that is not listed be used or if other modifications are made to existing BMPs, the efficiencies can be changed manually via the corresponding overrides. The user can override the existing value of a landscape or structural BMP from the *C* or *P*

overrides that reset to 1.0 after each addition. This value is analogous with *to do nothing*. If the input value is less than 1.0 and greater than 0.0, it will replace the appropriate BMP efficiency. If the value is not within that range, it will reset to 1.0, and the BMP selected will take precedence.

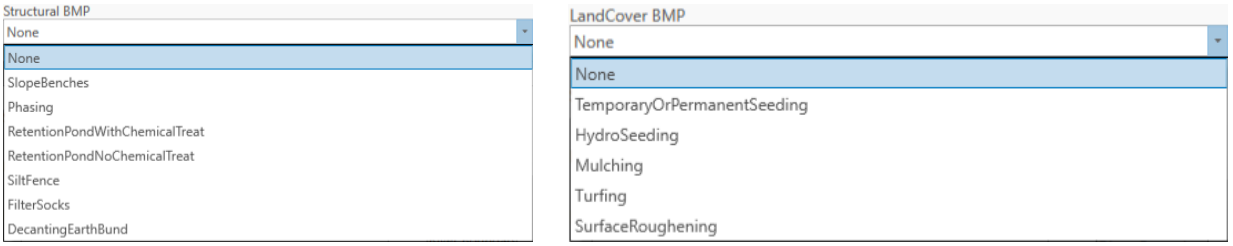

(**a**) (**b**)

Figure 4. Pre-assembled commonly used construction BMPs available in the GIS toolkit: (**a**) Structural BMPs, and (**b**) Landscape BMPs.

3.4. Rainfall Data

Rain gauge stations are scattered throughout a watershed and are generally more concentrated around major population centers. In addition, the precipitation data are continually being updated with new information. Because of climate change, a static weather model may not be ideal. Therefore, the National Oceanic and Atmospheric Administration (NOAA) Global Historical Climatology Network (GHCN) [41] will be used by the GIS toolkit to retrieve historical records from gauging stations within a set distance from the construction site centroid and will be processed to produce parameters for a 2-parameter gamma distribution. The Pearson Type III distribution, based on a 3-parameter gamma distribution, is widely used in hydrology [42]. The primary use of the third parameter is to have a lower bound that is not located at zero [43]. Since rainfall has a lower bound of zero, the 2-parameter gamma distribution was selected as a suitable substitution, following the work by [44,45]. The rainfall data will be used to produce a random distribution matching the weather statistics of the region being considered. The output will be used as the input for rainfall across the construction site for the SCS flow calculation approach.

3.4.1. Rain Gauge Station Selection

The GIS toolkit selects the appropriate rain gauge station in two major steps. First, a list of available gauges is retrieved from the NOAA GHCN database [41]. Then, a bounding box described by the latitude and longitude pairs of 36.6°, 25.8°, −93°, −107°, respectively, is utilized to select the gauges within the boundary. The current year at runtime (in the GIS toolkit) is retrieved from which two values are produced: the maximum start date of record and the minimum end date of record. In the developed model, these are described as at least 50 years from the current year and at most records ending 5 years from the current year.

After the rain gauge stations have been selected, a basic point distance formula (Equation (8)) will be used to find the closest gauge to the centroid of the construction site.

$$d = \sqrt{(x_1 - x_2)^2 + (y_1 - y_2)^2} \quad (8)$$

where d is distance, x_1 and y_1 are the rain gauge site latitude and longitude, and x_2 and y_2 are the construction site latitude and longitude. All distances are measured in decimal degrees (DD).

Because of the Earth's ellipsoidal shape, the distance between lines of latitude is not identical; however, the spacing between the lines of latitude at the equator and poles change by less than 1.6 km. For this application and narrow extent, the change was considered negligible. The closest site is then used to retrieve the rain gauge data from the NOAA GHCN database [41].

3.4.2. Rainfall Synthesis Methodology

This section explains how the data obtained from the rain gauge station closest to the construction site is used to develop a synthetic rainfall time series. Some simplifying decisions, such as only considering full record years, are made to enable automating the fitting of data to a two-parameter gamma distribution.

It is not appropriate to simulate a time series event by using consecutive single day design storms; therefore, an alternate standardized and reasonably repeatable method is required. To achieve that, each month was individually analyzed, synthesized, and merged with the previous monthly time series, which are equivalent to a 2%, 50%, and 75% chance of monthly occurrences. Those probabilities correspond to the 98th, 50th, and 25th percentiles, which are the required format for the statistical package.

An observation set comprised of n years of daily data for each month will be collated, then a Markov analysis will be performed. The analysis involves finding the probabilities of having *consecutive rainy-days*, *consecutive dry-days*, *a rainy-day followed by a dry-day*, and *a dry-day followed by a rainy-day*. These values will be counted and divided by their total counts to form a 2×2 probability matrix. The critical probabilities will be determined using a linear algebra solver. The two values represent the probability of rain or no rain for a given dataset and account for both the raw number of wet or dry days and the consecutive occurrences of each. Both the initial 2×2 probability matrix and stable state probabilities are shown for the Navasota River Bridge site and the month of January 2021 in Table 1.

Table 1. Probability and Stable State Matrices for the Navasota River Bridge Site, Texas, U.S. (33°14′00 to 33°14′30 N; 96°43′25 to 96°44′20 W) and the Month of January 2021.

State	Dry	Wet
Dry	0.821	0.179
Wet	0.617	0.383
Stable state	0.775	0.225

The gamma distribution parameters will be fit to the observed data using the sums of the individual monthly rainfalls, and the target values for the total monthly rainfall will be determined for the time series probabilities outlined above. The Python package, *scipy.stats.gamma.fit*, is used to fit the parameter, then an individual gamma distribution fitting of only rainy days will be performed. The sample size will be calculated by using the standard deviation of the total monthly rainfall (σ) and Equation (9). In this equation, the value of 1.26 corresponds to a 90% confidence level and an allowable error of 7 mm rainfall from the observational mean.

$$n_{samples} = \left(\frac{1.26\ \sigma}{7} \right)^2 \tag{9}$$

The variable $n_{samples}$ defines the number of random gamma distributions produced. These distributions are the product of rainy days and are therefore representative of potential values if rain occurs each month. A list of random values ranging from 0 to 1 is then produced and evaluated against critical probabilities mentioned previously. If the random value exceeds the probability of a *dry-day*, the random value is redefined to 1. If the random value does not exceed the probability of a *dry-day*, the value is redefined to 0. Each random rainfall distribution is multiplied by its own set of redefined random probabilities. The result is a synthetic rainfall time series that respects the local rainfall probabilities and the rainfall volume for a month-specific single event. These time series are $n_{samples}$ large per month.

Finally, the sums of the $n_{samples}$ time series are compared against the target monthly rainfall sums. The target monthly rainfall sums are produced by fitting a gamma distribution to the individual observed monthly rainfall sums. Then, the target percentiles are input into the distribution; the target monthly sums are output, and those that are closest to

the targets are selected for each probability range. Both the synthetic rainfall volume and *rainy-day* occurrence are confined but random events. Through the sample size calculation, a statistically reasonable number of random time series can be generated to reflect the target sums from the observation data. After the initial production of these synthetic time series, they are only referenced and not reproduced for each consequent construction activity in a simulation. A synthetic rainfall generated for the Wilson Creek bridge construction site, Texas, U.S. is presented in Figure 5.

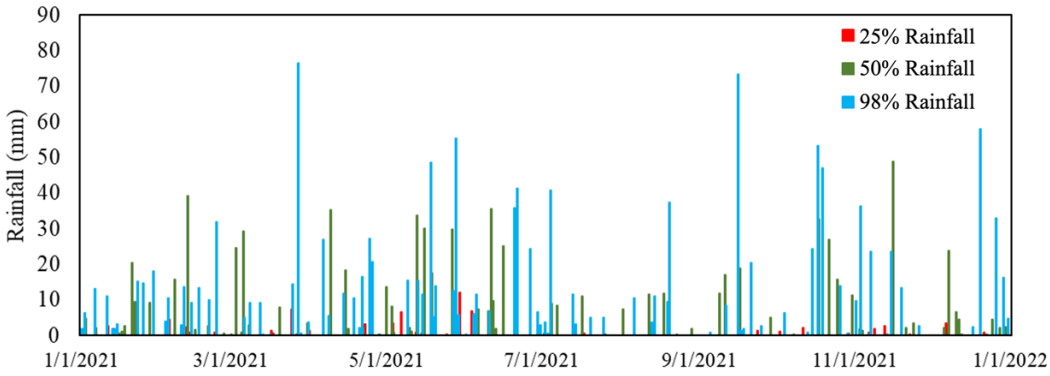

Figure 5. Synthetic rainfall time series generated by the overland erosion model for the Wilson Creek bridge construction site, Texas, U.S.

4. Study Area

The Wilson Creek bridge construction site on highway FM 2478 between the town of Prosper and the city of McKinney, Texas, U.S. was selected to evaluate the performance of the overland erosion model. The bridge is part of a roadway expansion project that is expanding the two-lane highway to six lanes. The construction of the bridge was proposed in two phases: a northbound bridge was constructed in Phase I, and the southbound bridge was completed in Phase II. Figure 6 shows the location of the bridge construction site and the nearby gauge stations.

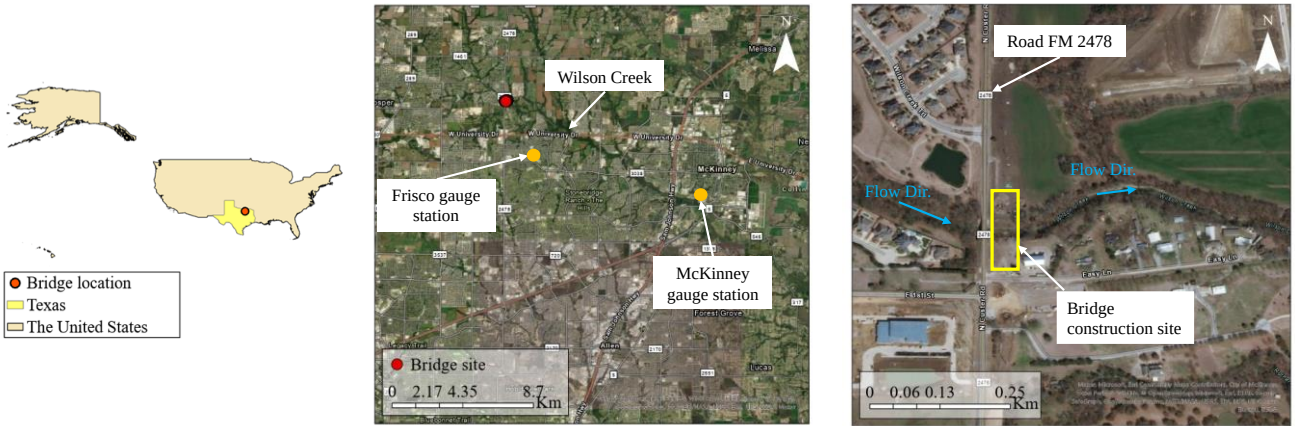

Figure 6. Wilson Creek bridge construction site on highway FM 2478, McKinney, Texas, U.S. and nearby precipitation and discharge gauge stations.

The Wilson Creek watershed originates in Collin County and is 196.8 km^2. The creek is 46.6 km long and discharges into Lavon Lake, which is located on the East Fork of the Trinity River. The bedrock in the Wilson Creek watershed consists of Austin chalk [46]. Wilson Creek lies within the Blackland Prairie, which expands through North Texas to the southwest of San Antonio [47] and is dominated by swelling clay soils (*Vertisols* according to the World Reference Base for Soil Resources (WRB)) that are prone to widescale surface erosion [48]. The land use in the watershed is comprised of residential and undeveloped

agricultural areas. Flow in the upper part of the creek is intermittent but becomes more perennial in its lower reaches due, in part, to runoff from municipal water uses [49].

The Wilson Creek watershed is in a humid subtropical climate area characterized by hot and humid summers and mild to cool winters. The temperature typically varies from 2 °C to 35 °C. The prevailing winds are from the south for 10 months; however, strong winds from the north can occur frequently in January and February. The average mean hourly wind speeds are the highest in March (19 km/h) and the lowest in August (13 km/h).

The weather stations closest to the Wilson Creek bridge construction site are the Frisco USC00413370 and McKinney US1TXCLL026 stations. The Frisco station is located 7.2 km southwest of the construction site, and the McKinney station is 12.9 km southeast (Figure 6). The rainfall data recorded at the Frisco station was selected in this study because of its closer proximity to the bridge sites and based on field observation, better represents the rainfall amount and timing at the construction site. The historical maximum, mean, and minimum annual precipitation at this station are 1850, 1013, and 592 mm. Rain is the dominant precipitation type in the watershed, and on average Frisco receives 25 mm of snow per year. The precipitation data recorded at Frisco and McKinney stations between December 2020 and December 2021 is shown in Figure 7. In 2021, a total of 1041 mm of precipitation was recorded at the Frisco station.

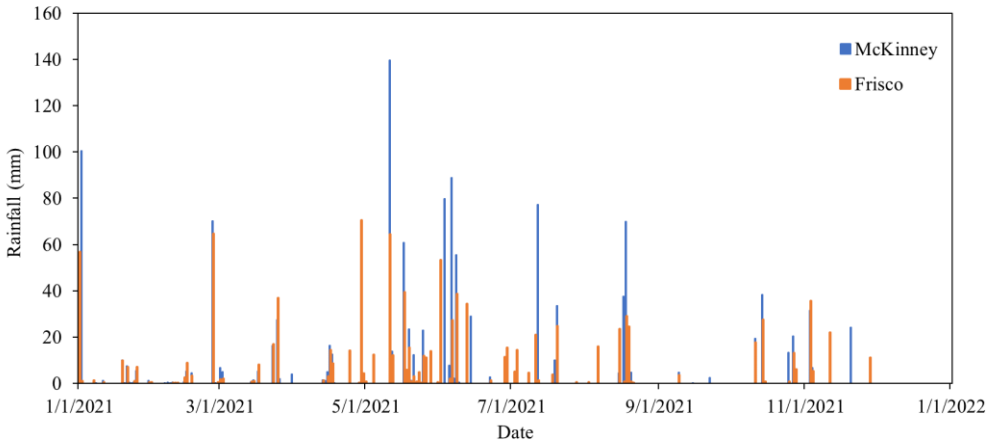

Figure 7. Rainfall data at McKinney and Frisco stations, Texas, U.S. in 2021.

5. Field Monitoring

The overland erosion was monitored at the Wilson Creek bridge construction site, and four 3 m × 3 m erosion plots were installed in February 2021 on the north and south sides of the creek, downstream of the bridge location (Figure 8a). The plots were constructed on different slopes, soil conditions, and surface covers based on the available space near the construction site. The components of the plots were the conveyance unit, storage tank, filtering mesh, and boundary (Figure 8b). The erosion plot was constructed to collect sediment moving towards the creek during storm events. Sediment deposited in the storage tank of each plot was collected after each storm from March to December 2021 and was sent to the lab for weight measurement and particle size analysis. The weight of the sediment was used to estimate the soil loss from the bounded area in each plot. The measured overland erosion data were compared with the result from the GIS toolkit overland erosion model to evaluate its performance.

Erosion Plot 1

Erosion Plot 1 was constructed on the south side of the creek (Figure 9a). The ground surface was vegetation-free and consisted of very fine to very coarse materials. The average surface slope inside the plot was 5.4%. Plot 1 was used for estimating the erosion of undisturbed soil from March to May 2021. Six overland erosion sediment samples were collected and analyzed from this plot.

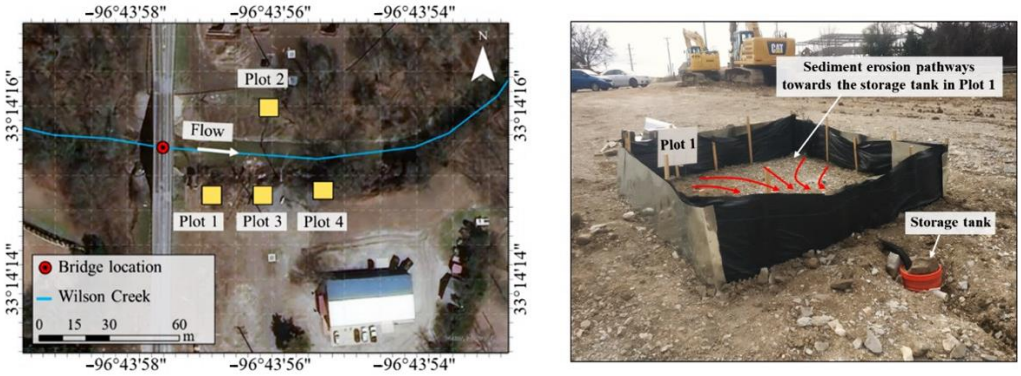

(**a**) (**b**)

Figure 8. (**a**) Location of erosion plots on the north and south sides of Wilson Creek downstream of the bridge location, and (**b**) Erosion plot No.1 and its components.

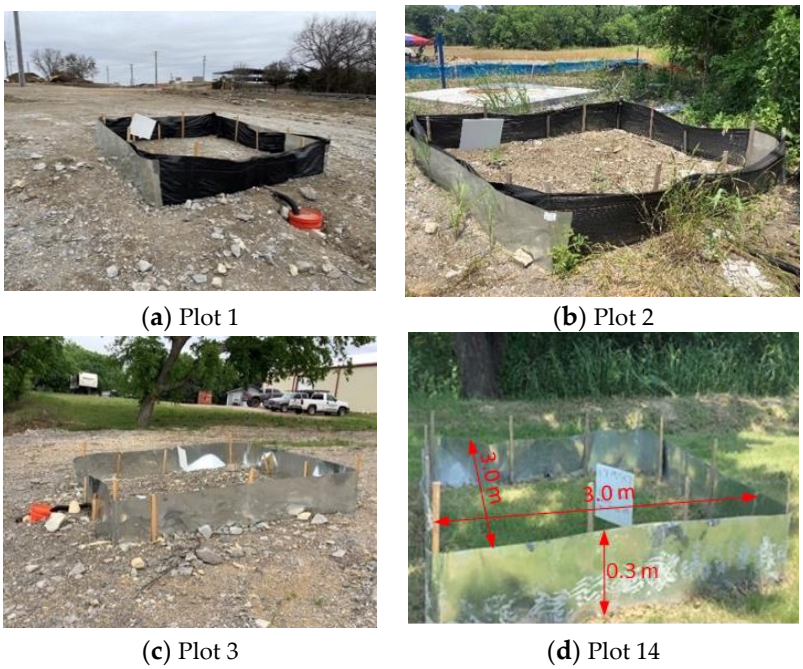

(**a**) Plot 1 (**b**) Plot 2

(**c**) Plot 3 (**d**) Plot 14

Figure 9. Erosion plots installed at the Wilson Creek bridge construction site (all plots were 3 m × 3 m × 0.3 m).

Erosion Plot 2

Plot 2 was constructed on the north side of the creek (Figure 9b). The ground surface was vegetation-free and consisted of very fine to very coarse materials. The topsoil in this plot was much more compact than that in Plot 1. The average slope inside the plot was 5.9%. Plot 2 was used for collecting the overland erosion from undisturbed surface conditions until May 2021, after which it was used for collecting soil erosion data from disturbed surface conditions. The topsoil inside the plot was raked during each visit to disturb the soil. Seventeen samples were collected and analyzed from this plot.

Erosion Plot 3

In April 2021, Plot 3 was constructed beside Plot 1 on the south side of the creek before Plot 1 was removed (Figure 9c). This plot was also constructed in a vegetation-free area with the same soil type as Plot 1. The average slope inside Plot 3 was 10.4%. This plot was used to collect the samples from disturbed and undisturbed soil surface conditions. The topsoil was raked during each visit, and eroded material samples were collected until June

2021. Plot 3 was removed after the implementation of slope protection BMPs at the end of June 2021. Five samples were collected and analyzed from Plot 3.

Erosion Plot 4

Plot 4 was constructed on the south side of the creek in an area with vegetative cover (Figure 9d). The eroded soil samples obtained from Plot 4 were compared with the sediment obtained from other plots constructed in areas with no vegetation. The average slope of Plot 4 was 7.3%. Eight samples were collected and analyzed from this plot.

The erosion plots were visited after each rainfall event. They were inspected regularly, and the sediment in the storage tanks was collected and measured to determine the amount of soil loss from the erosion plots during the storm event. A total of 36 sediment samples were collected from 4 erosion plots during the monitoring period and were transferred to covered, watertight containers to prevent leakage or spillage. They were then transported to the lab, where they were filtered to separate the sediment particles from the sediment-water mixtures, dried, and weighed to obtain the weight of soil loss from the plots during a storm event. They were filtered, using Whatman filter papers that were 15 cm (6 inches) in diameter with a pore size of 2.5 microns. The filtered samples were dried in an oven at 105 °C before the dry weight was measured.

The content of gravel, sand, silt, and clay in the sediment samples was measured by gradation and hydrometry tests. A gradation analysis was performed according to the American Society for Testing and Materials (ASTM) standard procedures [50] to classify the soil collected from the erosion plot. Several U.S. standard sieves ranging from No. 4 (4.75 mm) to No. 200 (75 μm) were used to determine the soil grain size.

A hydrometry test was conducted for the portion of the sediment sample that passed through sieve No. 200. The soil was mixed thoroughly with dispersing agents and water and poured into a cylinder with additional water. A hydrometer was used to take readings at specific time intervals. The result of the hydrometry test was combined with those of the sieve analysis for a complete gradation curve of the material or just for the fine material.

The data obtained from the recorded rainfall data at the Frisco rain gauge station (Figure 7) and the dry weight of sediment deposited in storage tanks were used to develop relationships between the rainfall amount and soil loss from erosion in Plots 1 to 4. These relationships are plotted in Figure 10. In developing these relationships, the dry weight of the sediment was plotted against the cumulative rainfall amount recorded between two site visits. For example, between the time when Plot 1 was installed and the first visit on 2 March 2021, there were four rainfall events with amounts of 65, 0.5, 1.8, and 2 mm. The cumulative rainfall for this period was 69.3 mm, which was plotted against the 1568 g of sediment collected during this visit. The relationships between the sediment yield and the rainfall show a moderate correlation with R^2 of 0.6 and 0.5 for Plots 1 and 4 and a higher correlation with R^2 of 0.8 for Plots 2 and 3. Figure 10 shows that plots with steeper slopes of trend lines were more susceptible to overland erosion. Plot 1 and Plot 4 showed the highest and lowest amounts of surface erosion during the monitoring period, respectively. Plot 4 was covered with native vegetation; therefore, a low erosion rate was expected. Plots 1 and 3 were constructed side by side; however, Plot 3 showed a lower erosion rate even though its soil surface was frequently disturbed by raking. Plot 3 was constructed on a much steeper surface than Plot 1 (10.4% vs. 5.4%). Plot 2 had the same slope as Plot 1, but it exhibited a lower erosion rate than Plot 1, even though it was raked frequently. The more compact soil on the north side of the construction site could be the reason for the moderate erosion rate in this plot. It should be noted that due to the limited length of the erosion plots, the runoff might have reached the plot outlet very quickly before forming concentrated flows. Thus, the erosion process in this plot might have been only due to the sheet flow.

The gradation curves of the eroded soils from each plot during the monitoring period are shown in Figure 11a–d. The eroded soils were primarily composed of clay, silt, sand, and a small percentage of gravel; the D_{50} of samples collected from each plot varied from 0.3 to 0.9 mm. No significant difference in the composition of eroded soils from Plots 1 to 4

was observed. A representative gradation curve for each plot was developed by averaging all gradation curves of that plot. The representative gradation curves for Plots 1 to 4 are shown in Figure 11e.

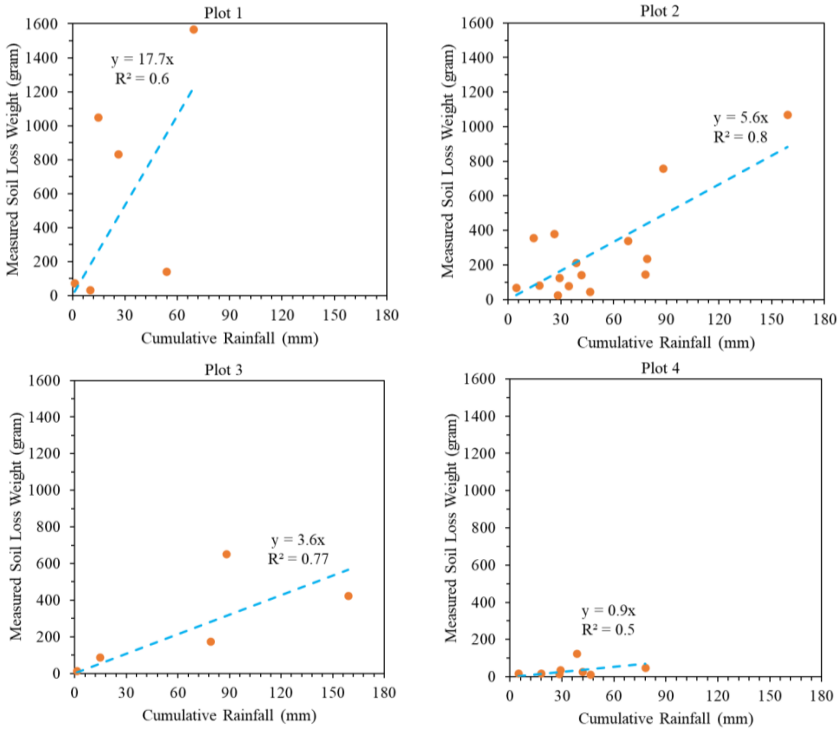

Figure 10. Relationship between the soil loss weight and cumulative rainfall depth from storms that occurred between two site visits to erosion Plots 1 to 4.

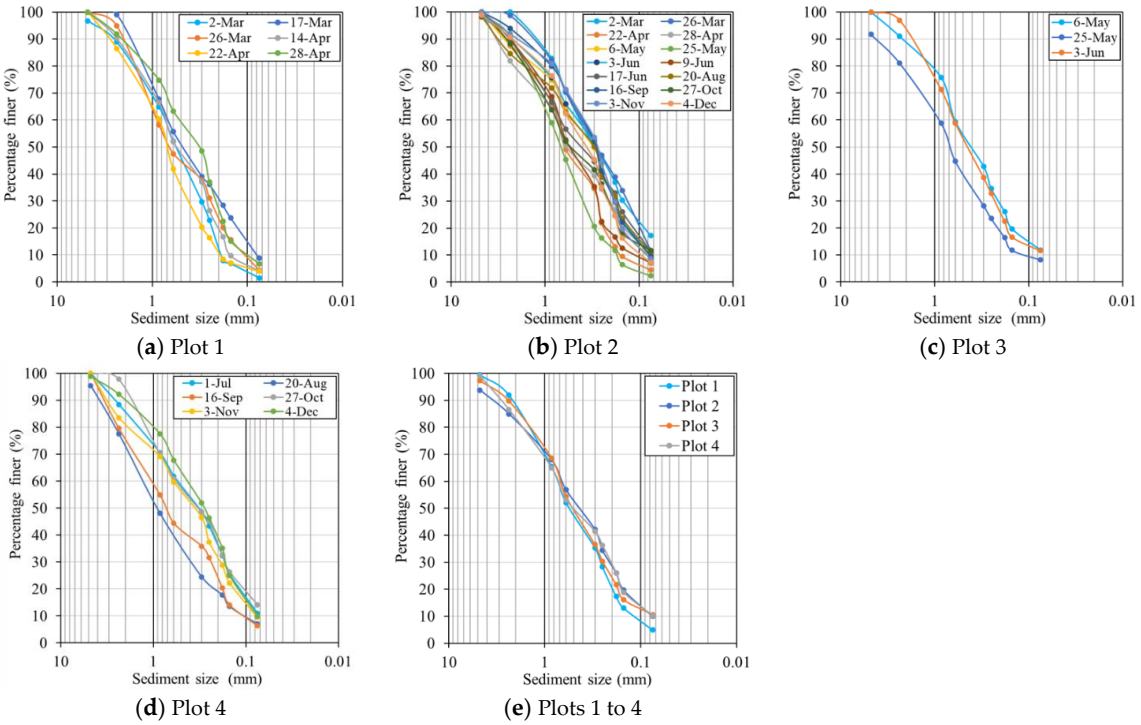

(**a**) Plot 1 (**b**) Plot 2 (**c**) Plot 3

(**d**) Plot 4 (**e**) Plots 1 to 4

Figure 11. (**a**–**d**) Gradation curves of eroded soils from erosion Plots 1 to 4 during the monitoring period of March to December 2021, and (**e**) Representative gradation curve for Plots 1 to 4. The dates represent the site visits when the samples were collected from the plots.

6. Wilson Creek Bridge Construction Site Overland Erosion Model

The overland erosion at the Wilson Creek bridge construction site was estimated for two scenarios: without-construction and with-construction. The without-construction scenario was simulated to evaluate the general performance of the model in predicting the natural erosion and sedimentation process in the study area. Neither construction activities nor BMPs were considered, as the lack of construction activity meant that the site's DEM, *CN*, and *K* were unchanged and there was no need for BMPs, as the site condition remained the same during the modeling period. Other inputs to the model, such as project footprint and rainfall were the same for both scenarios. The with-construction scenario was considered to assess the bridge construction effects on overland erosion and to compare the model results with the field data and observations.

Model Setup

The GIS toolkit estimates overland erosion using the MUSLE equation, which requires information about the watershed characteristics and rainfall, as broadly discussed in Section 3. Implementing the MUSLE in a geospatial format, however, requires different raster and vector input variables that are prepared by an automated iteration system. This section discusses the use of the geospatial input and intermediate datasets that were produced by the overland erosion model (OEM) for the Wilson Creek bridge construction site. Figure 12 illustrates the calculation steps used by the MUSLE-based overland erosion model and its six computational layers. These layers are discussed in the following.

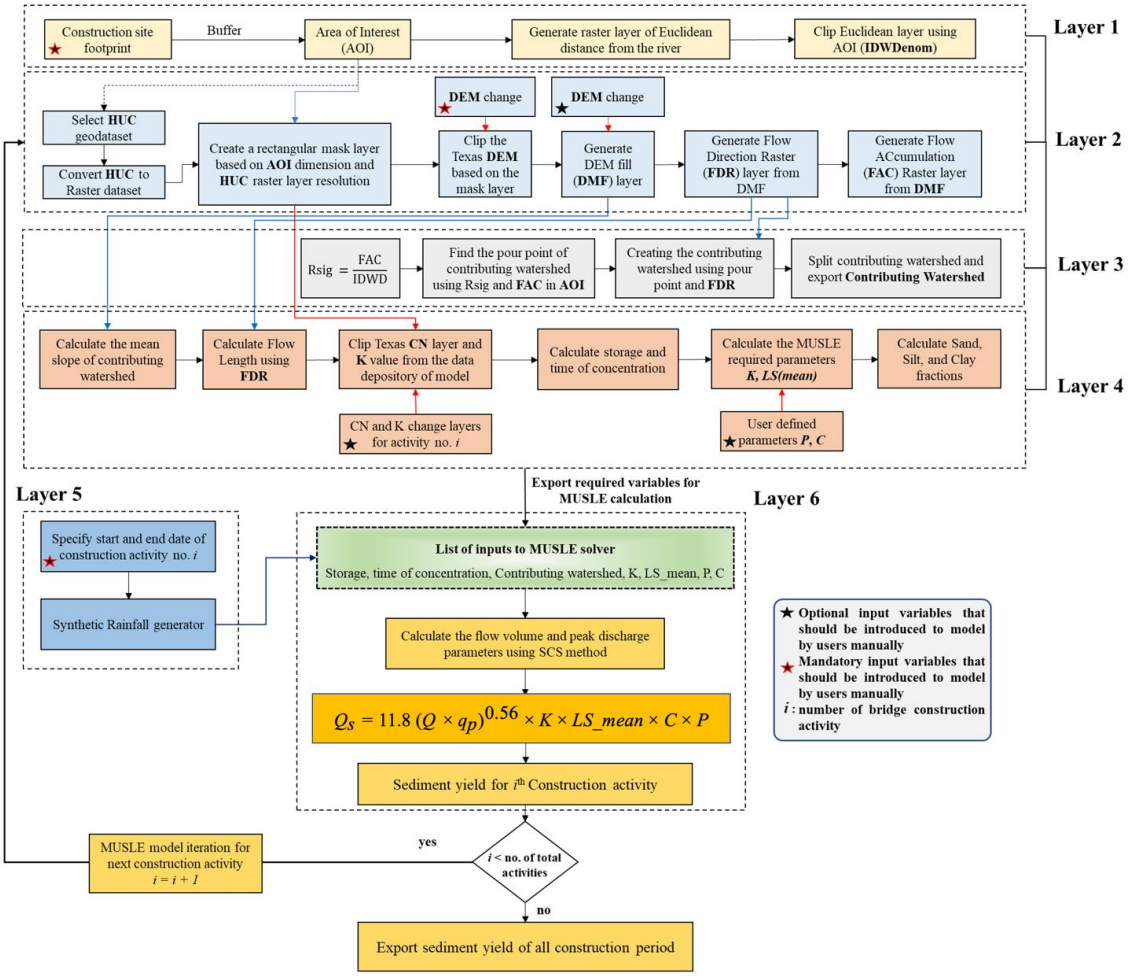

Figure 12. Calculation process of the GIS toolkit overland erosion model, based on the MUSLE method.

Layer 1: Site Footprint

The user manually-created bridge construction site footprint and the buffer analyst tools from the Arcpy package will be used to generate the construction site's area of interest (AOI) for the overland erosion model. Arcpy is a library that is used to produce automated geospatial calculations on the raster and vector input variables. The model generates a buffered layer based on the construction footprints covering the entire construction site, and the buffered layer is used as the main layer for clipping the required dataset in the MUSLE model. Users must manually produce the construction site footprint, and the model will automatically generate the AOI, based on a predefined buffer size. The size of the buffer zone is a function of DEM resolution, i.e., 10 m in this study.

The Wilson Creek construction site footprints were created based on field observations and are illustrated in Figure 13a. The total area of the footprints on the north side of the construction site is 1552 m^2 (16,705 ft^2) and on the south side is 2349 m^2 (25,284 ft^2). The footprint was considered the same for both the with- and without-construction scenarios.

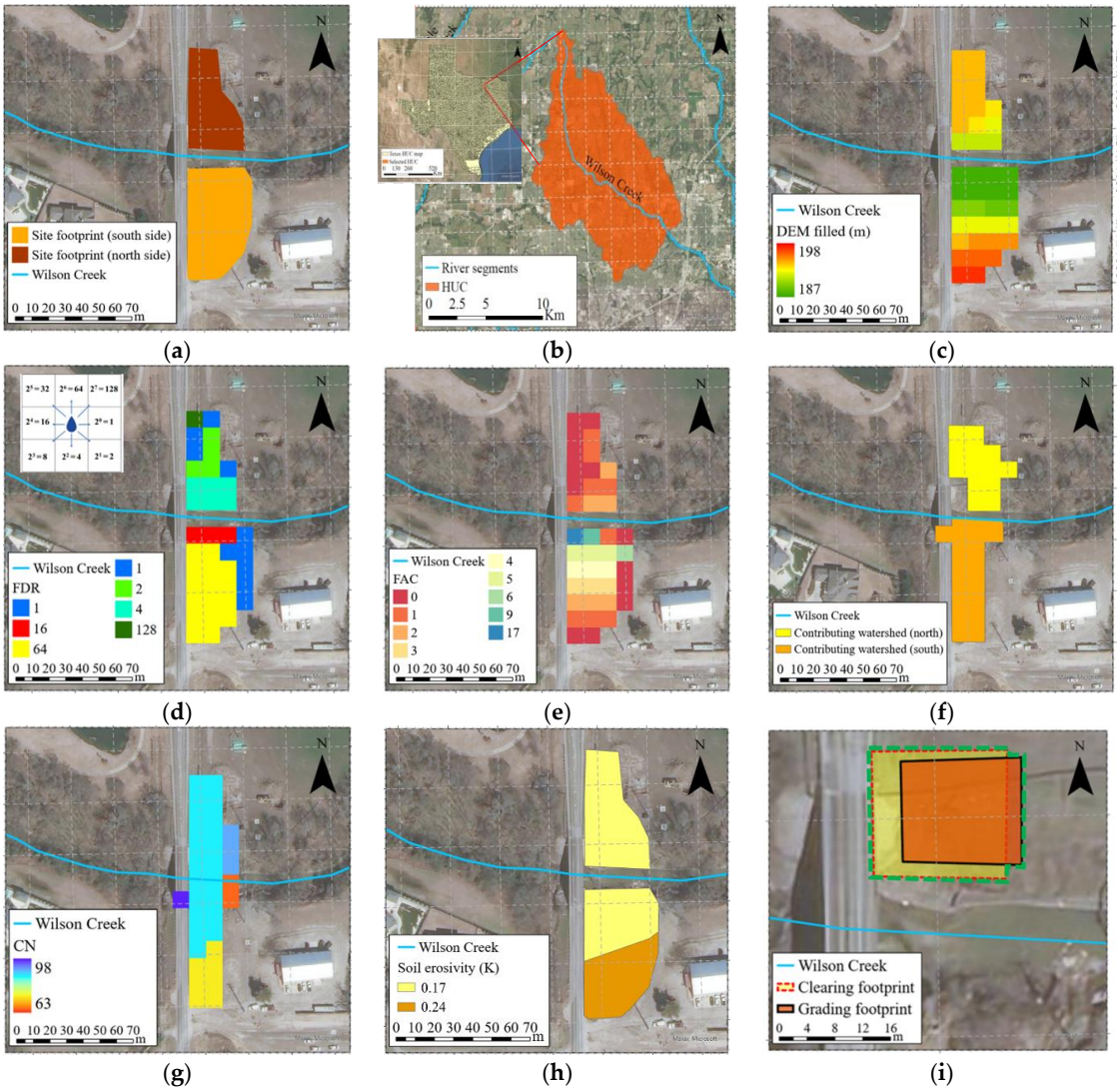

Figure 13. Wilson Creek (**a**) north and south bridge construction site footprints, (**b**) Texas HUC pieces used as repository dataset and selected watershed (HUC-12) for Wilson Creek by the model, (**c**) digital elevation model (DMF), (**d**) flow direction (FDR), and flow direction (FDR) values for eight different directions around a cell in raster dataset, (**e**) flow accumulation (FAC), (**f**) contributing watersheds, (**g**) curve number (*CN*), (**h**) soil erosivity factor (*K*), (**i**) footprint of clearing and grading activities in the north construction used in the calculation of weighted average soil erosivity factor (*K*).

Layer 2: Sub-watershed Selection Process

After introducing the construction site footprints, the centroid of these areas will be calculated by the model and the nearest sub-watershed (HUC-12) from the watershed depository dataset stored in the GIS toolkit package will be selected. Figure 13b shows the Wilson Creek watershed determined by the model. The selected watershed zonal coordinates (x_{min}, x_{max}, y_{min}, y_{max}) delineate the DEM corresponding to the study area on a larger scale. The DEM of the study area should be introduced manually by the user (the DEM layer for Texas is provided in the toolbox installation files) and stored as a pre-requisite file in the model's setup package. Once the DEM has been imported to the model, it is delineated, using a hypothetical rectangle that is based on the watershed's zonal coordinates. The delineated DEM is used in the spatial analysis fill toolbox to clean up the DEM from local depressions (sinks) before clipping it to a smaller area based on the site footprint. The DEM-filled (DMF) is the base layer that generates the flow direction and flow accumulation maps discussed in the following. Figure 13c shows the delineated DMF based on the site footprint. The construction site elevation ranged from 187 m (613.5 ft) to 198 m (649.6 ft). Since the DEM was not changed significantly due to the construction activity, the DMF was considered the same for both with- and without-construction scenarios.

The OEM uses the DMF to create the flow direction (FDR) and flow accumulation (FAC) raster datasets, based on the construction site footprint. Figure 13d shows the FDR raster dataset for Wilson Creek that was generated using spatial analyst tools in the Arcpy Python package. In a raster cell of flow direction, a drop of water can move in eight different directions. The inset in Figure 13d shows the possible directions for the water in each cell and the corresponding number representing the flow direction (FDR). The flow direction raster map identifies the cumulative number of cells that flow into each cell. A concentrated flow has a higher value of flow accumulation (FAC). Figure 13e illustrates the flow accumulation (FAC) maps for Wilson Creek's northern and southern construction sites. The flow direction (FDR) and flow accumulation (FAC) directly affect the area of the contributing watershed and the average slope length factor (*LS_mean*), calculated in Layers 3 and 4, respectively.

Layer 3: Creating Contributing Watershed

The third layer of the OEM uses the FAC and AOI to find the pour point of the contributing watershed on each side of the construction site. Once the pour point is defined, the watershed generator toolbox in the Arcpy spatial analyst tools can be used to generate the contributing watershed of the bridge construction site, using the FDR and pour point location. The OEM delineates the appropriate contributing watershed, based on the buffered construction site footprints. Figure 13f shows the contributing watersheds for the north and south sides of Wilson Creek. The contributing watershed area significantly affects the sediment yield generated by the MUSLE model. The delineated contributing watershed for the south part is estimated as 1735 m^2 (18,675 ft^2), while the north side contributing watershed area is calculated as 1378 m^2 (14,832 ft^2).

Layer 4: Calculating Hydrologic and Watershed Components

The overland erosion model produces buffered site footprints, DMF, FAC, FDR, and the contributing watershed geospatial variables required to calculate the sediment yield, using the MUSLE method. In Layer 4, the OEM uses geospatial datasets from Layers 1 to 3 to collect the appropriate hydrologic and watershed components from the depository dataset and the DEM-generated slope of the contributing watershed. The FDR is used to delineate the curve number (*CN*) and soil erosivity factor (*K*) from the depository dataset. Figure 13g shows the delineated *CN* map, where it can be seen that the *CN* values ranged from 63 to 98. The OEM used an average value of *CN* for each side of the creek to calculate the runoff volume. The *CN* map shown in Figure 13g was produced for the pre-construction condition and does not reflect any construction activity. The changes to *CN* caused by construction activities were introduced to the model at this step as a homogeneous raster dataset.

The soil erosivity factor (K) was used to produce the K map for the construction site footprints on the north and south sides of the creek, as shown in Figure 13h. For the without-construction scenario, the average value of K for the north side was 0.17, and for the south side was 0.20. It should be noted that the south side soil consists of two *erosivity* classes, including K = 0.17 for areas close to the stream and K = 0.24 for up-bank areas (Figure 13h). The model uses the invert distance weight function to calculate the impact of each soil class and to estimate the average K value, which was approximately equal to 0.20 for the south side.

Construction activities change the K value of the construction site. The overland erosion model is designed to consider a single value as the average K for the entire affected area for each construction activity. For example, Figure 13i shows the activity footprint for site clearing on the north side of Wilson Creek that covers an area of 338 m^2 (3638 ft^2). The grading activity footprint occurred after the site clearing, in an area of 251 m^2 (2701 ft^2). As shown in Figure 13i, the footprint of the grading activity overlaps with the site clearing footprint and requires the user to calculate a new K value based on the weighted average method and to introduce a single average K layer that represents the effect of all activities with overlap footprints. The green dash line in Figure 13i shows the merged area affected by grading and clearing with an average K value of 0.25. Since both activities have a K value of 0.25 in this project, the weighted average of K, in this case, is also 0.25. A weighted average K value was calculated for each construction activity for the entire site footprint on the north and south sides of the creek.

Layer 5: Construction Activity Duration and Rainfall Generator

The duration of each construction activity is introduced by entering its start and end date, and the BMPs that have been implemented may be introduced in this step. Bridge construction activities from 1 February 2021 to 31 November 2021 were considered and nine different activities were simulated. These activities and their durations are listed in Table 2.

Table 2. Wilson Creek Bridge Construction Activities and Implemented BMPs.

Construction Activity	Date		BMPs
	Start	End	
Site clearing	1 February 2021	10 March 2021	Silt fence-north side
Grading	11 March 2021	26 March 2021	Silt fence-north side
Temporary access road	27 March 2021	10 April 2021	Silt curtain and rock trap across the creek
Drilled shafts	11 April 2021	3 May 2021	Silt fence along the creek edge on both sides/Rock trap
Foundations/piers/abutments			Silt fence along the creek edge on both sides (after 15 May)/Rock trap (until 29 May)/Vegetation BMPs on the south side (from 3 June)
Southside	4 May 2021	2 June 2021	
Northside	3 June 2021	14 July 2021	
Backfilling	3 June 2021	14 July 2021	Silt fence along the creek edge on both sides/Vegetation BMPs on the south side
Slope formation	15 July 2021	29 July 2021	Vegetation BMPs on south side/Rock trap
Superstructure	30 July 2021	30 November 2021	Vegetation BMPs on south side/Rock trap

The GIS toolkit produces a set of synthetic daily time series that correspond to the 98th, 50th, and 25th percentiles of monthly rainfalls. Each time series is unique to that month, and the rain gauge is located near the construction site. The nearest rain gauge station to the Wilson Creek bridge site is the Frisco gauge station. In the present study, the recorded rainfall was exported from the Frisco precipitation gauge station, located 7.2 km southwest of the construction site, and imported to the model instead of producing synthetic rainfall scenarios to evaluate the overland erosion model performance.

Layer 6: MUSLE Model

A sediment yield calculation is iterated for each construction activity defined by the user. The sediment load tables are generated as the model outputs with corresponding sediment gradation, which are the required variables to run the in-stream sediment transport model of the toolkit.

7. Assessment of Overland Erosion Model Performance

The performance of the OEM for the Wilson Creek bridge site area was assessed by using the results from modeling the without-construction scenario and comparing them with the values estimated by other methods and field data. The start/end dates were entered into the toolkit from 1 January 2021 to 24 December 2021 as a one-year simulation period. Neither construction nor BMPs were considered, as the lack of construction activities meant that the site's DEM, *CN*, and *K* were unchanged and there was no need for BMPs, as the site condition remained the same during the modeling period.

7.1. Model Results for Without-Construction Scenario

The outputs of the OEM include sediment yield and gradation of the eroded materials. Figure 14 shows the rainfall events and the daily sediment yield from 1 January to 24 December 2021 for the north and south sides of the creek, as well as the combined sediment yield from both sides. It can be seen that the sediment yield from the south side was greater than that from the north side. The maximum estimated sediment yields from the north and south sides were 1.5 and 8.7 tons/day, respectively. The minimum sediment yield for the days with rainfall that caused soil erosion was estimated as 0.1 tons/day in total for both sides. The total annual sediment yields from the north and south sides were 9.3 and 42.6 tons/year, respectively, with corresponding *sediment yield per unit area* of 5.8 kg/m^2/year (23.3 tons/acre/year) and 18.6 kg/m^2/year (74.7 tons/acre/year), respectively.

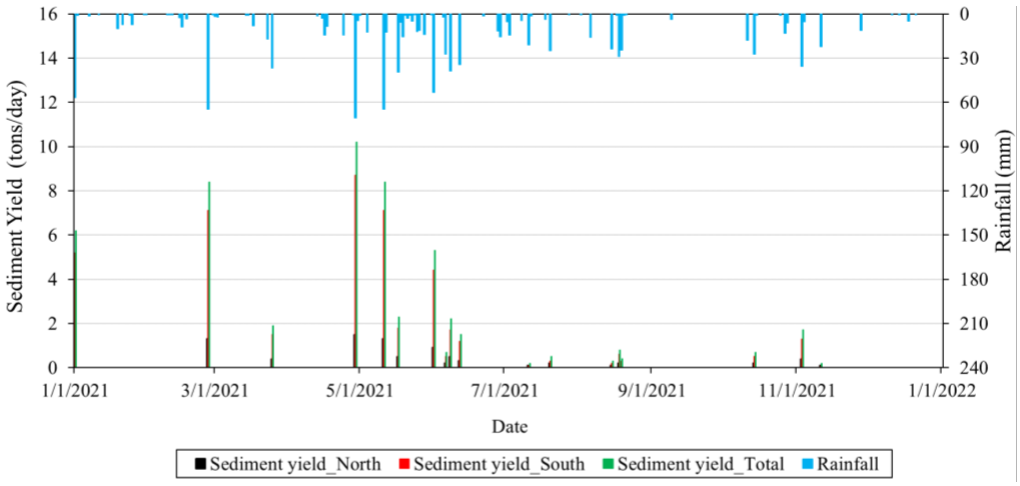

Figure 14. Sediment yield at the Wilson Creek bridge site for the without-construction scenario and daily rainfall records at the Frisco station.

Gradation of the eroded soil was also generated by the OEM for both the north and south construction sites. The soils were classified into three categories: sand, silt, and clay. Table 3 shows the fraction and average diameter of the soil particles for each side of the construction area.

Table 3. Fraction and Average Diameter of Eroded Soil Particles from the North and South Sides of the Wilson Creek Construction Site Developed by the OEM for the Without-construction Scenario.

Sediment Class	Ave. Diameter (mm)	Fraction (%)	
		North	South
Sand	0.25	9	10
Silt	0.016	21	32
Clay	0.002	70	58

7.2. Comparison with Universal Soil Loss Equation (USLE) Method

The soil loss for the north and south construction sites was calculated using the USLE method, which uses Equation (1) to calculate the annual soil loss rate due to rainfall. The rainfall erosive energy *R* for the Wilson Creek bridge site is 295 [22]. From Figure 13h, it can be seen that the average *K* values for the north and south construction sites are 0.17 and 0.19 (weighted average of 0.17 and 0.24), respectively. These values were extracted by the GIS toolkit from the SSURGO database. The average slope length factor (*LS*) was calculated by the GIS toolkit as 0.7 and 4.11 for the north and south sites, respectively. These values were confirmed by hand calculations and the table and graph presented in [22] for calculating the *LS* factor. Because no management practices and erosion controls were implemented in the without-construction scenario, the *C* and *P* values were taken as 1.0. The soil loss rates for the north and south construction sites calculated using Equation (1) were 8.7 kg/m^2/year (35.1 tons/acre/year) and 59.9 kg/m^2/year (242.5 tons/acre/year). The USEL equation parameters and estimated annual soil loss rates are summarized in Table 4.

Table 4. USLE Method Parameters and Estimated Annual Soil Loss Rate, Sediment Yield, and Sediment Delivery Ratio for Wilson Creek's North and South Construction Sites.

Site	*R*	*K*	*LS*	*C*	P	Soil Loss, *A* [1] (kg/m^2/Year)	Sediment Yield [2] (kg/m^2/Year)	Sediment Delivery Ratio (%)
North	295	0.17	0.7	1	1	8.7	5.8	66
South	295	0.2	4.11	1	1	59.9	18.5	31

[1] Calculated using Equation (1). [2] Estimated by the overland erosion model (OEM).

All of the eroded materials from a watershed may not enter streams or other waterbodies. The *sediment delivery ratio* is the ratio of the sediment yield (the portion of eroded material that enters the river or waterbody) to the total soil loss. In this study, the sediment yield was estimated by the OEM (Section 7.1), and the total soil loss was estimated using the USEL method (Table 4). The sediment delivery ratio for the north and south sides was 66% and 31%, respectively. The delivery ratio in areas with gully and streambank erosion is usually higher than that for sheet and rill erosion in up-bank areas, and since the Wilson Creek construction site is a mix of steep streambanks and areas with smaller slopes, the estimated sediment delivery ratios are within the ranges reported for Texas watersheds [51].

7.3. Comparison with Soil Loss from Erosion Plots

The sediment yields for the north and south construction sites were computed using the relationships developed between the rainfall and weight of the soil loss measured for Plot 1 (south side) and Plot 2 (north side), which are shown in Figure 10. The sediment yield for each day with recorded rainfall at the Frisco station, from 1 January to 24 December 2021, was calculated and totaled to obtain the annual sediment yield. The annual sediment yields for the north and south construction sites were estimated as 1 and 4.6 tons/year, respectively. These values are significantly smaller than estimated sediment yields by the OEM for the north and south sites, i.e., 9.3 and 42.6 tons/year. The reasons for such differences could be attributed to the plot size and soil conditions of the plots. Due to their limited length (3 m), runoff that developed inside the plots might have reached the outlet

quickly, before forming concentrated flows. Hence, the erosion process in the erosion plots might have just been due to the sheet flow. In addition, the soil conditions in each plot may not completely represent the entire construction site. For example, the surface slope of Plot 1 is 5.4%, while the average slope of the south construction site is 18%. The curve number (*CN*) for Plots 1 and 2 are 63 and 84, while this parameter varies between 48 and 86 on the south side and 84 to 89 on the north side (Figure 13g). Both the surface slope and the *CN* play significant roles in the volume of runoff, peak runoff discharge, and therefore the soil erosion rate. The soil erosivity factor (*K*) in Plot 1 (=0.17) is also different from the average *K* for the entire south construction site (=0.19) (Figure 13h). Despite the differences between the results from the OEM and erosion plots, however, both methods show that the annual sediment yield from the north site is 22% of the annual sediment yield from the south site.

8. Effects of Bridge Construction on Overland Soil Erosion

The OEM's estimates of the daily sediment yield from 1 January to 24 December 2021 are shown individually and collectively in Figure 15; the rainfall events are also shown in this figure. The contribution to the sediment yield was higher from the construction site in the south than from the north. The maximum estimated sediment yields from the north site and the south site and the total value from both sites were 1.7, 11.1, and 12.8 tons/day, respectively. These values correspond to 1.2, 6.4, and 4.1 kg/m^2/day. The minimum sediment yield for days with rainfall causing soil erosion was estimated as 0.1 tons/day for both sides. The total annual sediment yields from the north and south sides were 10.3 and 51.2 tons/year. These results show that the average sediment yield from the north and south construction sites increased by 11% and 20% because of construction activities. Figure 16 shows the period of each construction activity and compares the daily sediment yields for the north and south construction sites, for both the without-construction and with-construction scenarios. The total annual sediment yield from both sides was 61.5 tons/year (or 19.8 kg/m^2/year), which is 18.5% higher than the without-construction scenario's annual sediment yield.

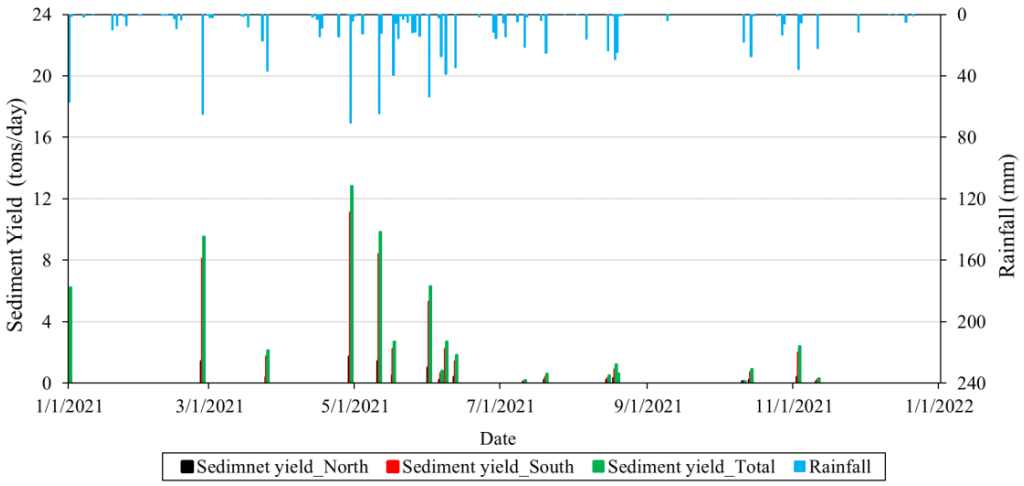

Figure 15. Sediment yield at the Wilson Creek bridge site due to overland erosion in construction areas and daily rainfall records from the Frisco station.

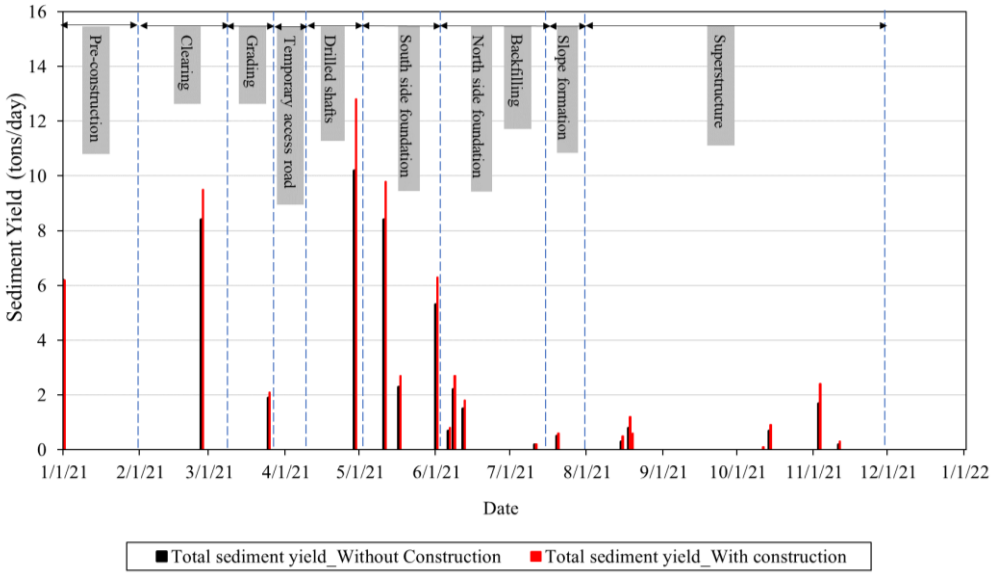

Figure 16. Comparison of with-construction and without-construction daily sediment yields at the Wilson Creek bridge site due to overland erosion and duration of construction activities.

9. Discussion

The developed GIS toolkit was set up for the Wilson Creek bridge site for two scenarios: without-construction and with-construction. A one-year simulation period, from 1 January 2021, to 24 December 2021, was selected for both scenarios, and the recorded rainfall for this period was used in the simulations. The without-construction scenario was performed to evaluate the toolkit performance in simulating overland erosion in the absence of any construction activities. The with-construction scenario simulation was conducted to assess the impact of bridge construction on overland erosion in Wilson Creek and compare the modeling results with the field data observations.

The overland erosion was monitored using erosion plots at the Wilson Creek bridge construction site, and data pertaining to the amount of rainfall was collected from the station closest to the construction site. The relationships developed between the amount of rainfall and the soil loss from erosion show that the erosion rate depends on the land cover, soil composition, degree of compaction, and length and slope of the overland flow path. The field data and observations provided information on the physical parameters, enabled the evaluation of the effects of bridge construction on overland erosion, and helped ground-truth the GIS predictive toolkit.

The performance of the OEM was evaluated by comparing the model results with the annual soil loss values estimated using the USLE method and field data. The application of the GIS toolkit in the Wilson Creek bridge construction site shows its potential in predicting the impacts of bridge construction projects on overland erosion.

9.1. Comparison with Soil Erosion from Other Construction Sites

The maximum increase in the daily sediment yield for the Wilson Creek construction site is estimated at 0.15 kg/m^2/day (north side), 1.38 kg/m^2/day (south side), and 0.83 kg/m^2/day (both sides). The sediment yield estimated for the north side is much smaller than the south side because of the smaller slope and soil erosivity factor *K* (Table 4). It is also comparable with the increase in the suspended sediment yield from a road construction site upstream of the Susquehanna River in Pennsylvania, U.S. where the increase in suspended sediment yield was measured as 3.85, 3.70, and 30 tons/h during three major construction activities. These values correspond to 0.085, 0.027, 0.1 kg/m^2/day [26].

The maximum increase in yearly sediment yield for the Wilson Creek construction site is estimated as 0.73 kg/m^2/year (north side), 5 kg/m^2/year (south side), and 3.1 kg/m^2/year (both sides). Similar to the maximum daily sediment yield, the increase

in annual sediment yield for the north side is much smaller than for the south side. The total sediment yield from both sides of the creek is comparable with reported values for the Pennsylvania Route 15 relocation and reconstruction, during which an additional 9100 tons of suspended sediment were introduced to the downstream creeks from the construction areas. The annual sediment yields due to construction activities in two watersheds in the project area were estimated between 2.8 and 3.9 kg/m^2/year [52].

9.2. Limitations of the Model and Future Direction

The toolkit is designed as an ArcGIS add-in with a pre-populated database for the state of Texas, U.S., but it can be used for any bridge construction site when the local database is imported. The performance of the toolkit was assessed using field data and observations at the Wilson Creek bridge construction site. The toolkit showed a promising performance; however, to reduce modeling uncertainties, develop an understanding of the uncertainties, and increase the accuracy of the approaches and model capabilities, the tool is to be applied at six bridge sites with a wide range of sediment characteristics.

Future research is required to assess alternative methods for defining eroded sediment characteristics from a typical construction site and to make recommendations for specific procedures that could be applied to bridge construction projects. The use of online soil databases, such as the SSURGO, has the advantage of ease of use but may not reflect conditions that have been altered from previous construction projects. Field sampling has the benefit of identifying more precise soil data but adds cost and requires standard procedures for the location and acquisition of the samples. Because the construction footprints for bridge projects are small compared to the scale of the soil surveys, field assessment of the soils may be required to determine accurate soil properties.

Future research will investigate using POLARIS soil data [53] in the toolbar instead of SSURGO. POLARIS is a probabilistic soil property map of 30 m over the contiguous U.S. It provides improved local prior distributions of soil parameters for land surface and hydrologic models. Soil sampling from six bridge sites will be collected to verify soil gradation obtained from SSURGO and POLARIS.

The soil erosivity K factor for the Wilson Creek bridge site (with-construction scenario) was selected based on judgment and values reported in a limited number of references. Future research can be performed to determine K for different soil types and conditions that represent typical bridge construction sites. Indoor or outdoor erosion plots can be designed and utilized for this purpose.

10. Conclusions

Eroded materials released from bridge construction sites may alter sediment regime and geomorphological conditions of receiving streams and may have short- and long-term impacts on aquatic habitats. Field monitoring and numerical modeling efforts have been reported in various road and bridge construction projects where attempts were made to assess the impacts that the construction might have on the stream sediment regime and aquatic habitats. However, no predictive model has been available to quantify the potential release of sediment during the construction of bridges. Therefore, a GIS-based Predictive Toolkit has been developed to estimate the overland erosion in bridge construction sites.

The preliminary evaluations showed promising results; however, the model needs to be applied to a large number of bridge construction sites to assess its performance in different settings and to increase its accuracy in estimating overland erosion and sediment yield.

Implementing the results of this research and utilizing the developed GIS toolkit will allow bridge design improvements that minimize the downstream effects and select effective BMPs. By applying this tool in bridge construction sites, transportation agencies and authorities may predict the project impacts and require contractors to implement measures to avoid or minimize such impacts.

Author Contributions: H.A. and M.P. conceptualized and designed the Overland Erosion Model (OEM). M.P. developed the OEM., S.K. and S.B. collected field data and performed the analysis. S.K. conducted laboratory testing, and X.Y. provided technical sight over fieldwork and laboratory testing. H.A. and M.P. drafted the manuscripts. All authors discussed the results and edited the manuscript. All authors have read and agreed to the published version of the manuscript.

Funding: This research was supported by the Texas Department of Transportation (TxDOT) under Project Number 0-7023, which was awarded to Habib Ahmari.

Data Availability Statement: Some or all field data, the toolkit, technical and user manuals, and an instructional video that was developed for this toolkit are available from the corresponding author upon reasonable request.

Acknowledgments: The authors are grateful for the support and technical guidance provided by the Texas Department of Transportation (TxDOT) Research and Technology Implementation's project team. Their assistance was central to the successful completion of this research project.

Conflicts of Interest: The authors declare no conflict of interest.

References

1. IHS Markit. Critical Infrastructure for Texas Growth. 2019. Available online: https://docs.txoga.org/files/1021-ihs_3-19-19-final.pdf (accessed on 26 August 2022).
2. U.S. Environment Protection Agency (EPA). *Environmental Impact and Benefits Assessment for Final Effluent Guidelines and Standards for the Construction and Development Category*; EPA-821-R-09-012; U.S. Environment Protection Agency (EPA): Washington, DC, USA, 2009.
3. Witheridge, G. *Erosion and Sediment Control Field Guide for Road Construction-Part 1*; Catchments & Creeks Pty Limited: Brisbane, Queensland, Australia, 2017.
4. Wellman, J.C.; Combs, D.L.; Cook, S.B. Long-term impacts of bridge and culvert construction or replacement on fish communities and sediment characteristics of streams. *J. Freshw. Ecol.* **2000**, *15*, 317–328. [CrossRef]
5. Hedrick, L.B.; Welsh, S.A.; Anderson, J.T. Influences of high-flow events on a stream channel altered by construction of a highway bridge: A case study. *Northeast. Nat.* **2009**, *16*, 375–394. [CrossRef]
6. Weaver, W.; Hagans, D. Road upgrading, decommissioning and maintenance: Estimating costs on small and large scales. In Proceedings of the NMFS Salmonid Habitat Restoration Cost Workshop, Washington, DC, USA, 14–16 November 2000; National Marine Fisheries Service, National Oceanic and Atmospheric Administration, U.S. Department of Commerce: Washington, DC, USA, 2004.
7. Ahmari, H.; Randklev, C.R.; Jaber, F.; Yu, X.; Baharvand, S.; Pebworth, M.; Kandel, S.; Goldsmith, A.M. *Determining Downstream Ecological Impacts of Sediment Derived from Bridge Construction*; TxDOT Report No. 0-7023; Texas Department of Transportation: Downtown Austin, TX, USA, 2022.
8. Mendonça dos Santos, F.; Proença de Oliveira, R.; Augusto Di Lollo, J. Effects of Land Use Changes on Streamflow and Sediment Yield in Atibaia River Basin—SP, Brazil. *Water* **2020**, *12*, 1711. [CrossRef]
9. Németová, Z.; Honek, D.; Kohnová, S.; Hlavčová, K.; Šulc Michalková, M.; Sočuvka, V.; Velísková, Y. Validation of the EROSION-3D model through measured bathymetric sediments. *Water* **2020**, *12*, 1082. [CrossRef]
10. Sharma, K.D.; Singh, S. Satellite remote sensing for soil erosion modelling using the ANSWERS model. *Hydrol. Sci. J.* **1995**, *40*, 259–272. [CrossRef]
11. Zhang, Y.; Degroote, J.; Wolter, C.; Sugumaran, R. Integration of modified universal soil loss equation (MUSLE) into a GIS framework to assess soil erosion risk. *Land Degrad. Dev.* **2009**, *20*, 84–91. [CrossRef]
12. Ohio Department of Natural Resources (ODNR). *Ohio Mussel Survey Protocol. Division of Wildlife and U.S. Fish and Wildlife Service (USFWS)*; Ohio Ecological Services Field Office: Columbus, OH, USA, 2020.
13. Virginia Department of Game and Inland Fisheries (VDGIF) and the U.S. Fish and Wildlife Service (FWS). *Freshwater Mussels Guideline for Virginia*; 2018. Available online: https://dwr.virginia.gov/wp-content/uploads/mussel-guidelines-11-2018.pdf (accessed on 26 August 2022).
14. U.S. Fish and Wildlife Service (USFWS); Ecological Services and Fisheries Resources Offices and Georgia Department of Transportation; Office of Environment and Location. *Freshwater Mussel Survey Protocol for the Southeastern Atlantic Slope and Northeastern Gulf Drainages in Florida and Georgia*; 2008. Available online: https://www.fws.gov/sites/default/files/documents/Final-Mussel-Survey-Protocol-FL-GA-April-2008.pdf (accessed on 26 August 2022).
15. U.S. Fish and Wildlife Service Texas Ecological Services Field Offices and Texas Parks and Wildlife Department. *Texas Freshwater Mussel Survey Protocol*; 2021. Available online: https://www.fws.gov/sites/default/files/documents/2021_Texas_Freshwater_Mussel_Survey_Protocol.pdf (accessed on 26 August 2022).
16. Weaver, W.E.; Hagans, D.K. *Handbook for Forest and Ranch Roads: A Guide for Planning, Designing, Constructing, Reconstructing, Maintaining and Closing Wildland Roads*; Pacific Watershed Associates: Arcata, CA, USA, 1994.

17. U.S. Department of Agriculture (USDA). *Erosion and Sedimentation on Construction Sites, Soil Quality-Urban Technical Note*; No.1; Soil Quality Institute: Auburn, AL, USA, 2000.
18. Merritt, W.S.; Letcher, R.A.; Jakeman, A.J. A review of erosion and sediment transport models. *Environ. Model. Softw.* **2003**, *18*, 761–799. [CrossRef]
19. Alewell, C.; Borrelli, P.; Meusburger, K.; Panagos, P. Using the USLE: Chances, challenges and limitations of soil erosion modelling. *Int. Soil Water Conserv. Res.* **2019**, *7*, 203–225. [CrossRef]
20. Roose, E. *Land Husbandry-Components and Strategy*; FAO Soils Bulletin: Rome, Italy, 1996; Volume 70.
21. Construction General Permit. Proposed Construction General Permit (CGP) 2017. Available online: https://www3.epa.gov/npdes/pubs/cgp_appendixh.pdf (accessed on 17 October 2019).
22. Yang, C.T. *Erosion and Sedimentation Manual*; U.S. Department of the Interior, Bureau of Reclamation: Denver, CO, USA, 2006.
23. Brevik, E.C.; Pereira, P.; Muñoz-Rojas, M.; Miller, B.A.; Cerdà, A.; Parras-Alcántara, L.; Lozano-García, B. Historical Perspectives on Soil Mapping and Process Modeling for Sustainable Land Use Management. In *Soil Mapping and Process Modeling for Sustainable Land Use Management*; Elsevier: Amsterdam, The Netherlands, 2017; pp. 3–28.
24. U.S. Department of Agriculture (USDA). *Revised Universal Soil Loss Equation Version 2 (RUSLE2) (for the Model with Release Date of 20 May 2008)*; Science Documentation; USDA-Agricultural Research Service: Washington, DC, USA, 2013.
25. Smith, S.J.; Williams, J.R.; Menzel, R.G.; Coleman, G.A. Prediction of Sediment Yield from Southern Plains Grasslands with the Modified Universal Soil Loss Equation. *J. Range Manag.* **1984**, *37*, 295. [CrossRef]
26. Younkin, L.M. Effects of Highways Construction on Sediment Loads in Streams. In *Soil Erosion: Causes and Mechanisms: Prevention and Control*; Washington, DC, USA, 1973; Volume 135, pp. 82–93. Available online: http://onlinepubs.trb.org/Onlinepubs/sr/sr135/sr135-008.pdf (accessed on 17 October 2019).
27. Reed, L.A.; Ward, J.R.; Wetzel, K.L. *Calculating Sediment Discharge from a Highway Construction Site in Central Pennsylvania*; U.S. Geological Survey, Pennsylvania Water Science Center: New Cumberland, PA, USA, 1985. [CrossRef]
28. Bouraoui, F.; Dillaha, T.A. ANSWERS-2000: Runoff and Sediment Transport Model. *J. Environ. Eng.* **1996**, *122*, 493–502. [CrossRef]
29. Morgan RP, C.; Quinton, J.N.; Smith, R.E.; Govers, G.; Poesen JW, A.; Auerswald, K.; Chisci, G.; Torri, D.; Styczen, M.E. The European Soil Erosion Model (EUROSEM): A dynamic approach for predicting sediment transport from fields and small catchments. *Earth Surf. Processes Landf. J. Br. Geomorphol. Group* **1998**, *23*, 527–544. [CrossRef]
30. Nearing, M.A.; Deer-Ascough, L.; Laflen, J.M. Sensitivity analysis of the WEPP hillslope profile erosion model. *Trans. ASAE* **1990**, *33*, 839–849. [CrossRef]
31. Neitsch, S.L.; Arnold, J.G.; Kiniry, J.R.; Williams, J.R. Soil and Water Assessment Tool Theoretical Documentation Version 2009. Texas A&M University System: College Station, TX, USA, 2011.
32. Sadeghi, S.H.R.; Gholami, L.; Khaledi Darvishan, A.; Saeidi, P. A review of the application of the MUSLE model worldwide. *Hydrol. Sci. J.* **2014**, *59*, 365–375. [CrossRef]
33. Williams, J.R.; Berndt, H.D. Sediment yield prediction based on watershed hydrology. *Trans. ASAE* **1977**, *20*, 1100–1104. [CrossRef]
34. Pongsai, S.; Schmidt Vogt, D.; Shrestha, R.P.; Clemente, R.S.; Eiumnoh, A. Calibration and validation of the Modified Universal Soil Loss Equation for estimating sediment yield on sloping plots: A case study in Khun Satan catchment of northern Thailand. *Can. J. Soil Sci.* **2010**, *90*, 585–596. [CrossRef]
35. Mays, L.W. *Water Resources Engineering*, 2nd ed.; John Wiley & Sons: Hoboken, NJ, USA, 2010.
36. U.S. Department of Agriculture (USDA). Revised Universal Soil Loss Equation 2-How RUSLE2 Computes Rill and Interrill Erosion. (n.d.). Available online: https://www.ars.usda.gov/southeast-area/oxford-ms/national-sedimentation-laboratory/watershed-physical-processes-research/research/rusle2/revised-universal-soil-loss-equation-2-how-rusle2-computes-rill-and-interrill-erosion/ (accessed on 17 October 2019).
37. Tillman, F.D.; Flynn, M.E.; Anning, D.W. *Geospatial Datasets for Assessing the Effects of Rangeland Conditions on Dissolved-Solids Yields in the Upper Colorado River Basin*; No. 2015-1007; U.S. Geological Survey: Washington, DC, USA, 2015.
38. U.S. Department of Agriculture (USDA). Soil Survey Geographic (SSURGO) Database. Available online: https://www.nrcs.usda.gov/wps/portal/nrcs/detail/soils/survey/geo/?cid=nrcs142p2_053631. (accessed on 26 August 2022).
39. Texas Commission on Environmental Quality (TCEQ) Open Data Portal. 2019. Available online: https://gis-tceq.opendata.arcgis.com/datasets/segments-poly?geometry=-154.658,24.504,-42.905,37.629. (accessed on 22 November 2019).
40. Texas Department of Transportation (TxDOT). TxDOT Roadways Inventory. Available online: https://gis-txdot.opendata.arcgis.com/datasets/843ebe994c114961a855ec76ddcde086_0/explore?location=31.061298%2C-100.081515%2C6.88. (accessed on 26 August 2022).
41. National Oceanic and Atmosphieric Adminestration (NOAA). National Centers for Environmental Information. Global Historical Climatology Network daily (GHCNd). Available online: https://www.ncei.noaa.gov/products/land-based-station/global-historical-climatology-network-daily. (accessed on 26 August 2022).
42. Singh, V.P. Pearson Type III Distribution. In *Entropy-Based Parameter Estimation in Hydrology*; Springer: Dordrecht, The Netherlands, 1998; Volume 30, pp. 252–274.
43. Grimaldi, S.; Kao, S.-C.; Castellarin, A.; Papalexiou, S.-M.; Viglione, A.; Laio, F.; Aksoy, H.; Gedikli, A. *Statistical Hydrology*; Wilderer, P.A., Ed.; Treatise on Water Science, Four-Volume Set (p. 488); Elsevier Science: Amsterdam, The Netherlands, 2011; pp. 479–517. [CrossRef]

44. Fadhil, R.; Rowshon, M.; Ahmad, D.; Fikri, A.; Aimrun, W. A stochastic rainfall generator model for simulation of daily rainfall events in Kurau catchment: Model testing. *Acta Hortic.* **2017**, *1152*, 1–10. [CrossRef]
45. Tettey, M.; Oduro, F.T.; Adedia, D.; Abaye, D.A. Markov chain analysis of the rainfall patterns of five geographical locations in the southeastern coast of Ghana. *Earth Perspect.* **2017**, *4*, 6. [CrossRef]
46. Ferring, C.R. Late Quaternary Geology of the Upper Trinity River Basin, Texas. Doctoral Dissertation, The University of Texas at Dallas, Richardson, TX, USA, 1994.
47. Moring, J.B. *Effects of Urbanization on the Chemical, Physical, and Biological Characteristics of Small Blackland Prairie Streams in and near the Dallas-Fort Worth Metropolitan Area, Texas*; Chapter C in Effects of urbanization on stream ecosystems in six metropolitan areas of the United States (No. 2006-5101-C); U.S. Geological Survey: Washington, DC, USA, 2009.
48. Harmel, R.D.; Richardson, C.W.; King, K.W.; Allen, P.M. Runoff and soil loss relationships for the Texas Blackland Prairies ecoregion. *J. Hydrol.* **2006**, *331*, 471–483. [CrossRef]
49. Maier, N.D.; Dunkin, J.T. McKinney Floodplain Management Study: Wilson Creek, Franklin Branch, Stover Creek, Honey Creek; Prepared for City of McKinney, Texas; 1988. Available online: https://www.mckinneytexas.org/DocumentCenter/View/408/McKinney-Floodplain-Management-Study-_1988?bidId= (accessed on 13 August 2022).
50. American Society for Testing and Materials (ASTM). *Standard Practice for Classification of Soils for Engineering Purposes (Unified Soil Classification System. s.l.*; ASTM International: West Conshohocken, PA, USA, 2006.
51. Greiner, J.H. *Erosion and Sedimentation by Water in Texas-Average Annual Rates Estimated in 1979*; Report Prepared for Texas; Department of Water Resources: Sacramento, CA, USA, 1982.
52. Hainly, R.A. *The effects of highway construction on sediment discharge into Blockhouse Creek and Steam Valley Run*; Pennsylvania (No. 80-68); U.S. Geological Survey: Washington, DC, USA, 1980.
53. U.S. Geological Survey (USGS). POLARIS: A 30-Meter Probabilistic Soil Series Map of the Contiguous United States. Available online: https://pubs.er.usgs.gov/publication/70170912 (accessed on 26 August 2022).